No. 53

The Mineral Exploration-
Mineral Deposits and Tectonics of
Two Contrasting Geologic Environments
in
The Republic of the Philippines

Consolidated Report on Northern Sierra Madre Area
•
Consolidated Report on Palawan Area

MARCH 1989

JAPAN INTERNATIONAL COOPERATION AGENCY
METAL MINING AGENCY OF JAPAN

MPN
CR (5)
89—29

The Mineral Exploration-
Mineral Deposits and Tectonics of
Two Contrasting Geologic Environments
in
The Republic of the Philippines

Consolidated Report on Northern Sierra Madre Area

•

Consolidated Report on Palawan Area

FEBRUARY 1989

JAPAN INTERNATIONAL COOPERATION AGENCY
METAL MINING AGENCY OF JAPAN

MPN
CR (5)
89-29

Preface

In response to the request of the Government of the Philippines, the Government of Japan has decided to conduct a survey on the potential of mineral resources in the eastern Luzon, Visayas and the Palawan. The survey was entrasted to the Japan International Cooperation Agency (JICA) and the Metal Mining Agency of Japan (MMAJ).

This Consolidated Report includes the results of synthesized regional analyses about the Northern Sierra Madre Area and Palawan Area which has been surveyed under the abovementioned works.

We wish to express our deepest appreciation to the officials of the Government of the Philippines and the Ministries of Foreign Affairs and International Trade and Industry of Japan and the officials of the Embassy of Japan for their close cooperation for the survey.

February, 1989

Kensuke Yanagiya
President
Japan International Cooperation Agency

Junichiro Sato
President
Metal Mining Agency of Japan

Consolidated Report on Northern Sierra Madre Area

SUMMARY

A total area of 9,785 km^2 in the Northern Sierra Madre was covered by geological and geochemical prospecting in 1986 as a part of the Mineral Exploration - Mineral deposits and Tectonics of Two Contrasting Geologic Environments in the Republic of the Philippines.

The results of the above were processed statistically with a regional perspective, and the results were evaluated comprehensively together with the results of the geological survey, mineral prospecting and the study of existing geoscientific data of the area.

The Northern Sierra Madre Area witch is located in the northern part of Luzon, is geologically divided into two zones, namely the eastern and western zones.

The eastern zone consists mainly of Cretaceous ophiolite while the western zone of Paleogene pyroclastics and Neogene sedimantary rocks, Oligocene diorite stocks intruded in the Paleogene pyroclastics. The border of the two zones is the Divilacan Thrust which dips westward. The ophiolite in the eastern zone is composed mainly serpentinized peridotite and partly accompanied by gabbro, basalt and Cretaceous chert. Neogene calcareous mudstone partly overlies these rocks unconformably.

The western zone is topographically subdivided into the mountainous part in the east and the basins in the west. The geology of the mountainous area consists of Paleogene andesitic-dacitic pyroclastics and diorite intruding into these pyroclastics. These volcanic clastics are the product of Paleogene calc-alkaline igneous activity of the area. Neogene basaltic volcanic rocks overlie the above igneous rocks unconformably and are distributed widely from the mountains to the basin area. Limestone and terrigenous clastic beds overlie them and the overall structure of the area is monoclinic with gently westward dipping.

Thus the lithology of the Northern Sierra Madre area changes, from east to west, from Cretaceous ophiolite, Paleogene calc-alkaline bodies and to gently dipping Neogene sediments. These three units are products of oceanic crust, magmatic arc and back arc basin respectively.

The major minelalization of the eastern zone is the orthomagmatic chromium concentration in periodotite, and the Cyprus type copper concentration in basaltic pillow lava.

The mineralization in the western zone is found in veins and dissemination of copper, lead, zinc sulfide in Tertiary andesite and the porphyry copper in the contact zone between diorite intrusive bodies and andesitic volcanic rocks.

The regional analysis and interpretation of the geochemical anomalies were carried out on 11 elements (Cu, Pb, Zn, Ag, As, Mn, Ni, Co, Mo, Hg and Cr) of approximately 5,000 stream sediment samples (less than 0.175 mm in diameter) collected in the area.

The whole surveyed area was divided into 2 km× 2 km cells and the following four statistical analyses were carried out using the geometric means of the contents of the 11 elements of the samples in each cell.

(1) Univariate analysis of the cell average values

(2) Univariate analysis of the moving average values which determines the average value of nine cells as the value of the central cell.

(3) Univarite analysis of high-pass filter values which is the positive difference between each cell average and moving average values.

(4) Multivariate analysis (Factor analysis) for the cell average values.

The results were represented in 1:1,000,000 scale maps (Attached plates PL-2-1 to PL-2-4).

These results were, then, evaluated together with the distribution of igneous bodies, geologic structure and alteration associated with mineralization.

Finally the following three localities were extracted as promising and warranting further prospecting (Attached plate PL-9).

I Vicinity of the Dimakawal mineral showing in the southeastern most of the western zone: In this zone Paleogene andesitic pyroclastics are distributed and diorite intrusive body is found near in the west side.
Assumed type of major mineralization and the associated commodities; hydrothermal veins and disseminated type mineralization of copper, lead, zinc sulfide. Cu, Pb and Zn.

II West side of Port Bicobian in the eastern coast of the eastern zone: The ultramafic rocks are distributed in this zone.
Assumed type of major mineralization and the associated commodities; Cyprus type copper mineralization. Cu, Zn, Mn and Cr.

III Upstream of Tuguegarao River in the northern part of the Central Mountain Range of the western zone: In this zone the lithological contact between the andesitic-dacitic pyroclastics of Paleogene age and diorite intruding into these pyroclastics is situated.
Assumed type of major mineralization and the associated commodities; Porphyry type copper mineralization. Cu and Zn.

The Mineral Exploration-Mineral Deposits and Tectonics of two Contrasting Geologic Environments in The Republic of The Philippines

Consolidated Report on The Northern Sierra Madre Area

Contents

List of Figures

List of Tables

List of Attached Plates

PL-2-4 (No. 1 to No. 5)
Geochemical Analysis Factor Analytical Values Distribution Map (1:1,000,000)

PL-3 Distribution Map of Anomalous Values in Panned Samples (1:1,000,000)

PL-4 Distribution Map of the Major Heavy Minerals Wt % in Panned Samples (1:1,000,000)

PL-5 Compiled Gravimetric Map (Bouguer Anomalies) (1:1,000,000)

PL-6 Lineaments Map (LANDSAT Images) (1:1,000,000)

PL-7 Locality Map of Mineral Showings (1:1,000,000)
Attached Index Table of Mineral Showings

PL-8 Index Map of Existing Data regarding Survey Works of the Area (1:1,000,000)

PL-9 Relation Map between Promising Area and Mineral Showings Localities (1:1,000,000)

Appendixes

Appendix 1 Histograms and Cumulative Frequency Curves of Cell average Values

Appendix 2 Flow Charts of Chemical Analysis

Appendix 3 List of the Existing Data

1. Introduction

1-1 Purpose and Scope

1-1-1 Background and Particulars

Pursuant to the Implementing Arrangement (I/A) entered into between the Government of the Philippines through the Mines and Geo-Sciences Bureau (MGB) and the Government of Japan through the Japan International Cooperation Agency (JICA) and the Metal Mining Agency of Japan (MMAJ) signed on September 26, 1984, a project officially titled "The Mineral Explorations-Mineral Deposits and Tectonics of Two Contrasting Geologic Environments" was carried out in the Republic of the Philippines.

This report embodies the results of the synthetic evaluation on the Northern Sierra Madre Area which is included in the abovementioned exploration project. The field survey took place from May to July in 1986 (JICA-MMAJ Report 1987).

1-1-2 Objectives of the Report

This report embodies the summary of the results of the survey and of the study of previous works regarding the mineral resources in the Northern Sierra Madre Area which is located in the northeastern part of the Republic of the Philippines.

The objectives of this report include the clarification of the mineral resources distribution in the survey areas through correlating, processing and analyzing all acquired data.

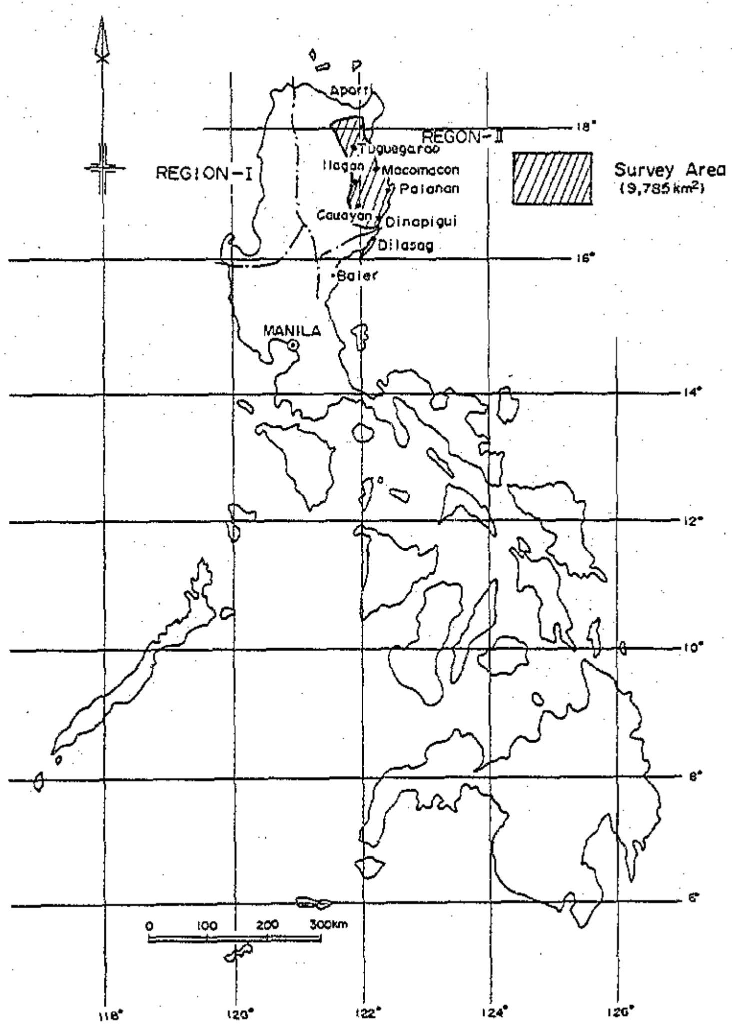

Fig. 1 Location Map of the Survey Area

1-2 Regional Setting (Ref. Figs. 1 and 3)

1-2-1 Location and Accessibility

The Northern Sierra Madre Area is located in the northeastern part of the Luzon Island of the Republic of the Philippines. The Northern Sierra Madre Range extends from north to south through the central part of the survey area forming a steep mountain ridge, the highest peak of which is Mt. Dos Curenos (1,850 m). The survey area is bordered by the divide that extends through latitude 18° 07' N in the north, the southern boundary of the Isabela Province which is at through latitude 16° 30' N in the south, the Cagayan River in the west and the eastern coastline of this area in the east. The total survey area is 9,785 km^2.

Most of this area belongs administratively, to the Isabelal Province of Region II, but the northern part of the area belongs to the Cagayan Province.

1-2-2 Access

A highway built along the Cagayan River connects Aparri which is in the northernmost part of the survey area, to Manila. It takes 10 hours by car to travel between Manila and Tuguegarao.

The access to the eastern coast is possible only by sea transport from Baler or Dilasag of Aurora Province.

Air transport is available from Cauayan along the Cagayan River to Dinapiqui (PATECO private airstrip), Maconacon (ACME private airstrip) and Palanan (public airstrip) by chartered aircraft.

The location and access is shown in Figures 1 and 3.

1-2-3 Climate and Vegetation

The climate of the eastern area of the mountain range belongs to a typical monsoon climate zone of the Western Pacific, where the dry season is from April to June, the typhoon season from July to October and the wet season from November to March. Annual precipitation is about 3,400 mm and average temperature is about 27°C.

The climate of the western area of the mountain range also belongs to the monsoon climate zone of the Western Pacific, where the dry season is from November to May and the wet season from June to October. Annual precipitation is about 1,700 mm and average temperature is about 27°C. During the wet season many typhoons pass across the area. The vegetation of the hilly areas between the lowland and the mountain range is mostly covered by virgin forests of mainly broad-leaved trees and bamboos. The main industries of this are area agriculture and forestry.

Most of the lowlands along the Cagayan River and its tributaries and coastal plains around Palanan of the east coast are planted with rice.

It was also noted that coral reefs are abundant along the east coast.

1-3 Personnel Involved

1-3-1 Planning and Negotiations

Japanese panel:

Takeshi Izumi	Metal Mining Agency of Japan (MMAJ)
Kyoichi Koyama	id
Hideo Hirano	id
Natsumi Kamiya	id
Yoshitaka Hosoi	id

Philippine panel:

L. T. Abuyuan	Department of Environment and Natural Resources (DENR)
G. R. Balce	Mines and Geo-Sciences Bureau (MGB)
R. M. Luis	id
E. G. Domingo	id
R. L. Almeda	id
N. V. Ferrer	id

1-3-2 Preparation of the Consolidated Report

Japanese Panel:

Yoshikazu Okubo	Overseas Mineral Resources Development Co. (OMRD)
Yukio Uehara	id
Yoshihiko Shimazaki	id
Akio Shida	Nittetsu Mining Consultants Co., Ltd.
Kazuyoshi Masubuchi	Dowa Engineering Co., Ltd.

Philippine panel:

R. M. Samaniego	Mines and Geo-Sciences Bureau (MGB)
M. V. Garcia	id
B. S. Vargas	id
R. M. Luis	id
R. L. Almeda	id
R. Villones	id
A. Apostol Jr.	id
M. A. Aurelio	id
R. A. Santos	id

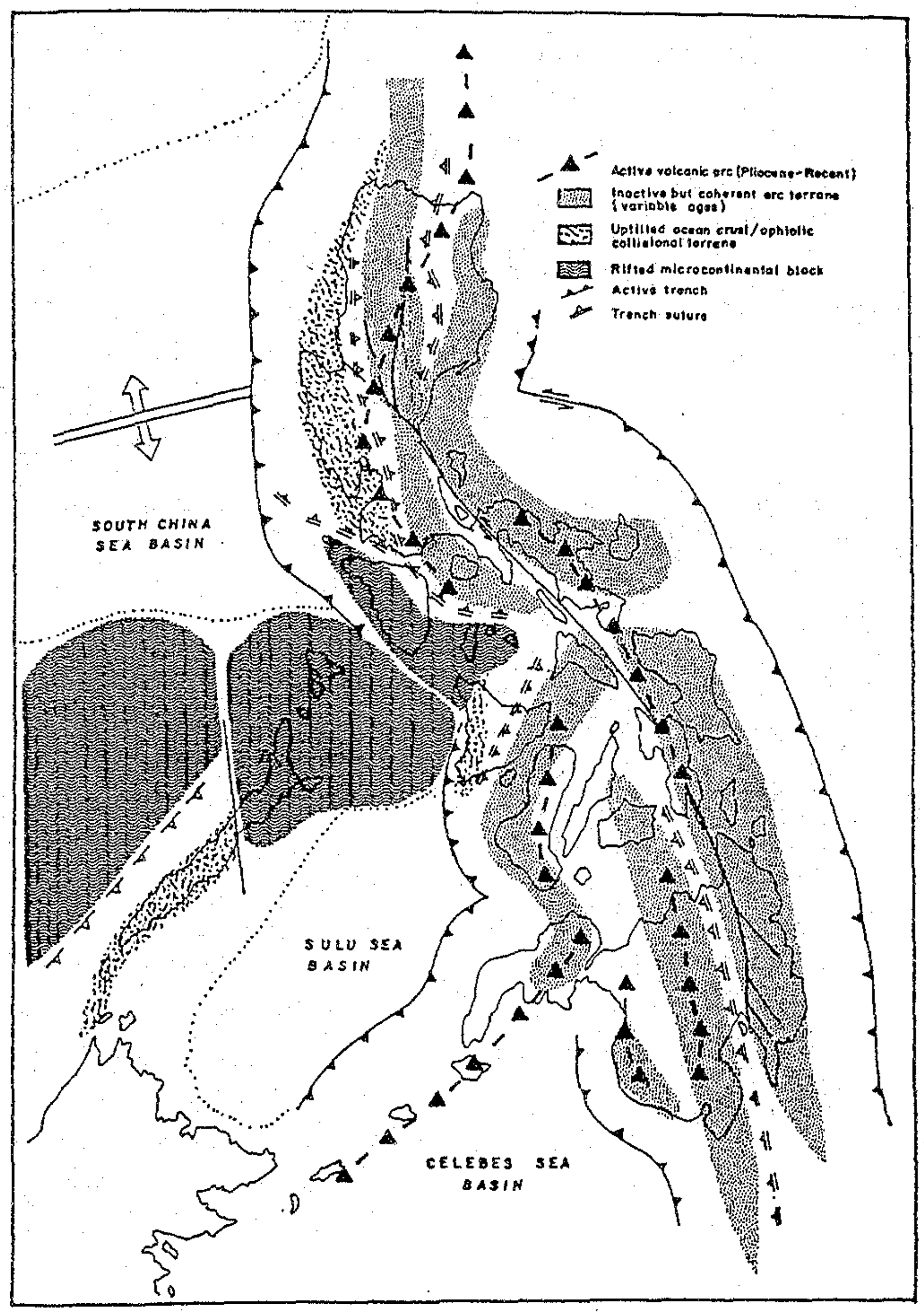

Fig. 2 Tectonic Terrans of the Philippines (After A. S. Zanoria et al. 1984)

1-4 Methodology

The analyses and interpretation of the geoscientific data from the Northern Sierra Madre area were conducted as follows:

1-4-1 Survey area (Figs. 3 and 4)

The survey area is divided geologically into two areas by the Divilacan Thrust, namely the Eastern part of the Northern Sierra Madre (hereafter called the Eastern Part) and the Western part of the Northern Sierra Madre (hereafter called the Western Part).

The Western Part is bordered by the Cagayan River in the west.

1-4-2 Stratigraphy (Figs. 5 - 6, and Attached plate-1.)

A geological Workshop held in Manila in June 1988 between the Japanese and Philippine panels come up with a stratigraphic classification that is used in report, during the workshop held in Manila in June, 1988 was used.

A geological map in the scale in 1:1,000,000 has been prepared in conformity with the stratigraphic classification.

1-4-3 Geochemical data

In terms of the geochemical data, the zones with anomalous values were identified utilizing the following processes:

The 4,973 stream sediment samples from Northern Sierra Madre were analysed for 11 elements; Cu, Pb, Zn, Ag, As, Mn, Ni, Co, Mo, Hg, Cr.

The survey area was divided into 2km × 2km cells. Univariate and multivariate analyses of the average values of all the cells were carried out. The univariate analyses of the moving average values of all the cells and of the high-pass filter values were also made. The high-pass filter values were calculated from the differences between the cell average and the moving average values.

1-4-4 Heavy mineral samples

In addition to the stream sediment samples, a total of 370 heavy mineral samples from the Northern Sierra Madre Area were collected by panning. Au, Ag and Ga analyses were conducted and the analytical data were treated by univariate analyses. Forty of the above samples were selected at random and the mode of component minerals were studied.

1-4-5 Existing data

Available existing data on previous geoscientific work of the area were compiled and are presented in the lineament map, gravity map, mineral showings distribution map and survey data index map.. These were compiled in 1:1,000,000 scale to conform with the geological, geochemical and other maps of this project. Most of these maps were printed in color.

The locations of previous geoscientific work of the area are shown in PL-8 and list of their works are attached in Appendix.

1-5 Achievements of the Project

1-5-1 Conclusions

Four principal mineralizations are found in the survey area; namely in the Eastern Part, the orthomagmatic mineralization which is the Ni and Cr concentration related to the differentiation process of peridotite of Isabela Ultramafic Complex in ophiolite zone and the Cyprus type massive sulfide copper mineralization occurs along the upper boundary of the pillow lavas of the Bicobian Basalt which is distributed in the western side of Port Bicobian.

While in the West Part, the sulfide vein and dissemination type mineralization which are observed in volcanic breccia of the Abuan Formation and the porphyry type copper mineralization which occurs along the contact between the dacitic (Mt Cresta Formation) to andesitic (Abuan Formation) rocks and the Northern Sierra Madre Batholith, are observed both in the Northern Sierra Madre mountain range.

The regional analysis and interpretation of geochemical anomalies were carried out on 11 elements of approximately 5,000 stream sediment samples collected in the area.

The results of the geochemical analyses were, then, evaluated together with the distribution of igneous bodies, geologic structure and alteration associated with mineralization.

As a result of the consideration of the abovementioned available informations, three promising areas were selected with following priorities.

In addition, the lenticular chromite mineralization associated with ophiolite was excluded from new promising zone because geochemical anomalies are concentrated in the vicinity of the operating Wasayan mine.

I Vicinity of the Dimakawal mineral showing in the southeastern most of the western zone: In this zone Paleogene andesitic pyroclastics are distributed and diorite intrusive body is found near in the west side.
Assumed type of major mineralization and the associated commodities; hydrothermal veins and disseminated type mineralization of copper, lead, zinc sulfide. Cu, Pb and Zn.

II West side of Port Bicobian in the eastern coast of the eastern zone: The ultramafic rocks are distributed in this zone.
Assumed type of major mineralization and the associated commodities; Cyprus type copper mineralization. Cu, Zn, Mn and Cr.

III Upstream of Tuguegarao River in the northern part of the Central Mountain Range of the western zone: In this zone the lithological contact between the andesitic-dacitic pyroclastics of Paleogene age and diorite intruding into these pyroclastics is situated.
Assumed type of major mineralization and the associated commodities; Porphyry type copper mineralization. Cu and Zn.

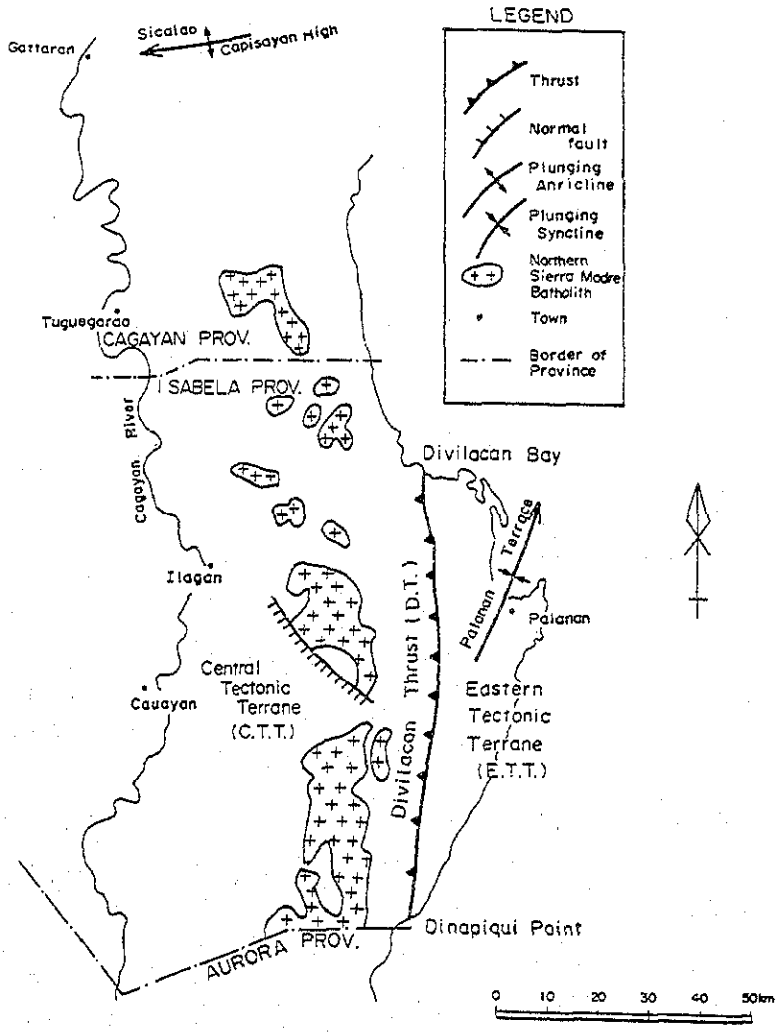

Fig. 3 Tectonic Division Map of the Northern Sierra Madre Area

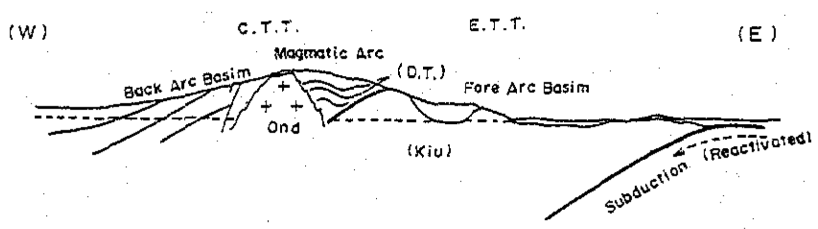

Fig. 4 Idealized Tectonic Profile of the Northern Sierra Madre Area

2. Geology and Mineralization

2-1 Geological Setting (Figs. 2, 3, 4 and Attached plate 1)

2-1-1 Regional Geology

The survey area is located at the northeastern part of the Philippine Archipelago and belongs to the Eastern Physiographic Province of the Philippine Mobile Belt.

The area is divided into two tectonic areas with the Divilacan Thrust as the tectonic boundary. This thrust trends N-S and is parallel to the Northern Sierra Madre Range on its eastern side.

2-1-1-1 The Eastern Part

This area belongs to the East Tectonic Terrane (Aurelio and Billedo, 1987.), where an ophiolite suite serves as the basement.

This ophiolite is the terrane which is believed to have been generated and formed in the Philippine sea.

Middle Miocene to Oligocene sedimentary rocks overlie the basement unconformably. They are believed to have been deposited in the forearc basin developed between the Northern Sierra Madre Range and the old East Luzon Trench which had previously existed in the east.

2-1-1-2 The Western Part

This area belongs to the Central Philippine Arc Terrane (McCabe et al., 1985) which is considered equivalent to the Central Tectonic Terrane (Aurelio and Billedo, 1987). This area is composed of the Northern Sierra Madre Range and the Cagayan Basin. The Northern Sierra Madre Range is a magmatic arc which extends southward and forms the Eastern Luzon Paleogene Diorite-Granite Intrusive Belt.

The southern extension of the Central and Eastern Tectonic Terranes has been cut by the Philippine Fault.

The oldest formation in this part of the survey area is the Abuan Formation of early Oligocene age and is exposed mainly in the Northern Sierra Madre Range.

The Oligocene Northern Sierra Madre Batholith consist of diorite to granodiorite, intruded into the Abuan Formation. Tectonic reconstruction led to the classification of the Cagayan Basin as a backarc basin where the post-Oligocene sedimentary rocks were deposited.

These rocks occupy a monoclinal belt with the beds dipping gently to the west in the survey area.

The idealized E-W direction profile of the survey area is shown in Fig. 4.

2-1-2 Stratigraphy

Stratigraphic sections agreed upon during the Workshop in Manila on June 1988 are shown in Figures 5 and 6.

2-1-2-1 The Eastern Part

The Isabela Ultramafic Complex, which is identified as the basement of this area, is extensively exposed along the eastern coast. It consists mostly of peridotite with minor amount of dunite lenses and massive and beded gabbro.

Ultramafic rocks which are usually serpentinized form the host rock of chromite ore deposits. The Isabela Ultramafic Complex has been thrust under the Dipadian Formation of the Western Part by the Divilacan Thrust.

The Bicobian Basalt and Dikinamaran Chert are distributed near Port Bicobian and the eastern coast of Palanan. They are deposited over the Isabela Ultramafic Complex. It is considerably difficult to clearly difine the stratigraphic relationship between the Bicobian Basalt, Dikinamaran Chert and Isabela Ultramafic Complex, because these formations are in thrust contact with each other as observed in the field.

The uppermost Dikinamaran Chert has been assigned Early Cretaceous age on the basis of Radiolarian identification.

The Bicobian Basalt is dark, massive and fine-grained. It occurs as pillow lava and are sometimes intercalated with the Dikinamaran Chert.

Dierico Formation consists of polymictic conglomerate and mudstone interbeds and is thought to be of Early Miocene age. This formation appears to have been deposited after thrusting since it overlies the thrust. It is found as small outcrops in the northern part of Dinapiqui Point and a similar but longer body is exposed along the upstreams of the Hang River.

The Palanan Sediments consist of semi-consolidated sandstone and calcareous mudstone. Sedimentation is throught to have occurred during the Late Miocene making the Palanan Sediments younger than the Dierico Formation.

The Palanan Sediments were deposited on the depression of the Isabela Ultramafic Complex exposed around Palanan.

The Kanaipang Limestone is generally massive and coralline. It conformably overlies the marginal part of the Palanan Sediments. This formation is assigned Pliocene to Pleistocene age.

2-1-2-2 The Western Part

The Abuan Formation is the oldest formation in the Western Part and is widely distributed in the Northern Sierra Madre Range. It consists of a heterogeneous mixture of basaltic to andesitic flows and brecciated basaltic to andesitic sediments and pyroclastics. The age of the deposition of the Abuan Formation is infered to be before Early Oligocene age.

The Dipadian Formation which forms the basement of this area together with the Abuan Formation, is exposed along the Divilacan Thrust on its western side. From the bottom, it consists of a well-indurated feldspathic wacke with intercalation of intraformational conglomerates.

On the upper portion of the wacker, well-bedded siltstone and mudstone were deposited. The Dipadian Formation contains thin-bedded limestone which yields foraminifera of Late Oligocene to Early Miocene age. The top part of this formation is transitional to the upper beds and contains thin greenish tuff, which is correlated to the Masipi Green Tuff.

The Mt. Cresta Formation is exposed typically on the mountain side of Mt. Cresta and lies scattered on the ridges of the Northern Sierra Madre Range. It is a dacitic complex of lava flows, intrusives, pyroclastics and sedimentary deposits.

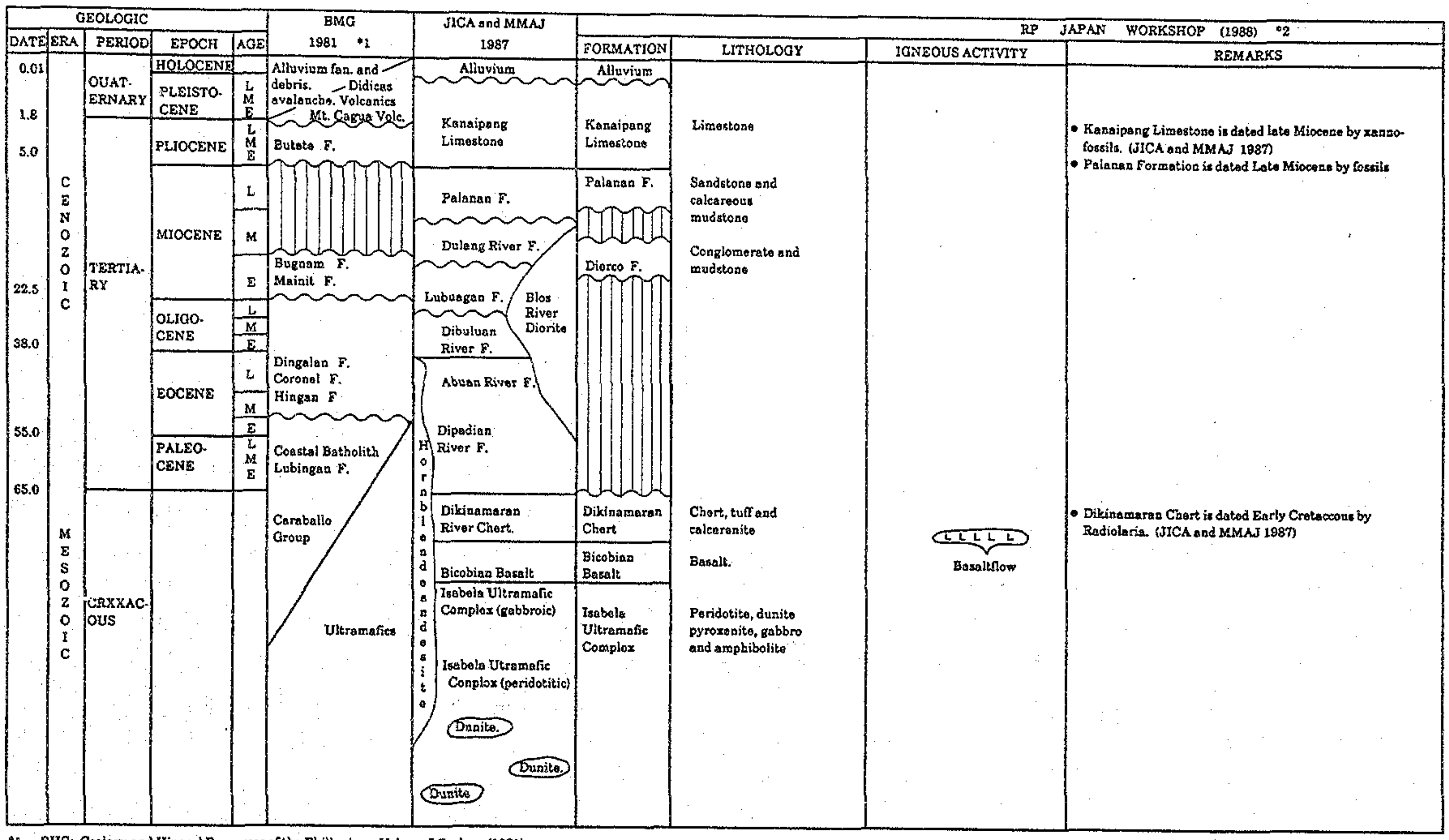

*1 BHG: Geology and Hineral Resources of the Phillupines, Volume I Geology (1981) p. 68 (Table II 31)
*2 M.A. Aurelio and E.B.Billedo. Tectonic Implications of the Geology and Hineral Resources of Northern Sierra Hadre. ms. (1987)

Fig. 5 Stratigraphic Column in the Eastern Part of the Area

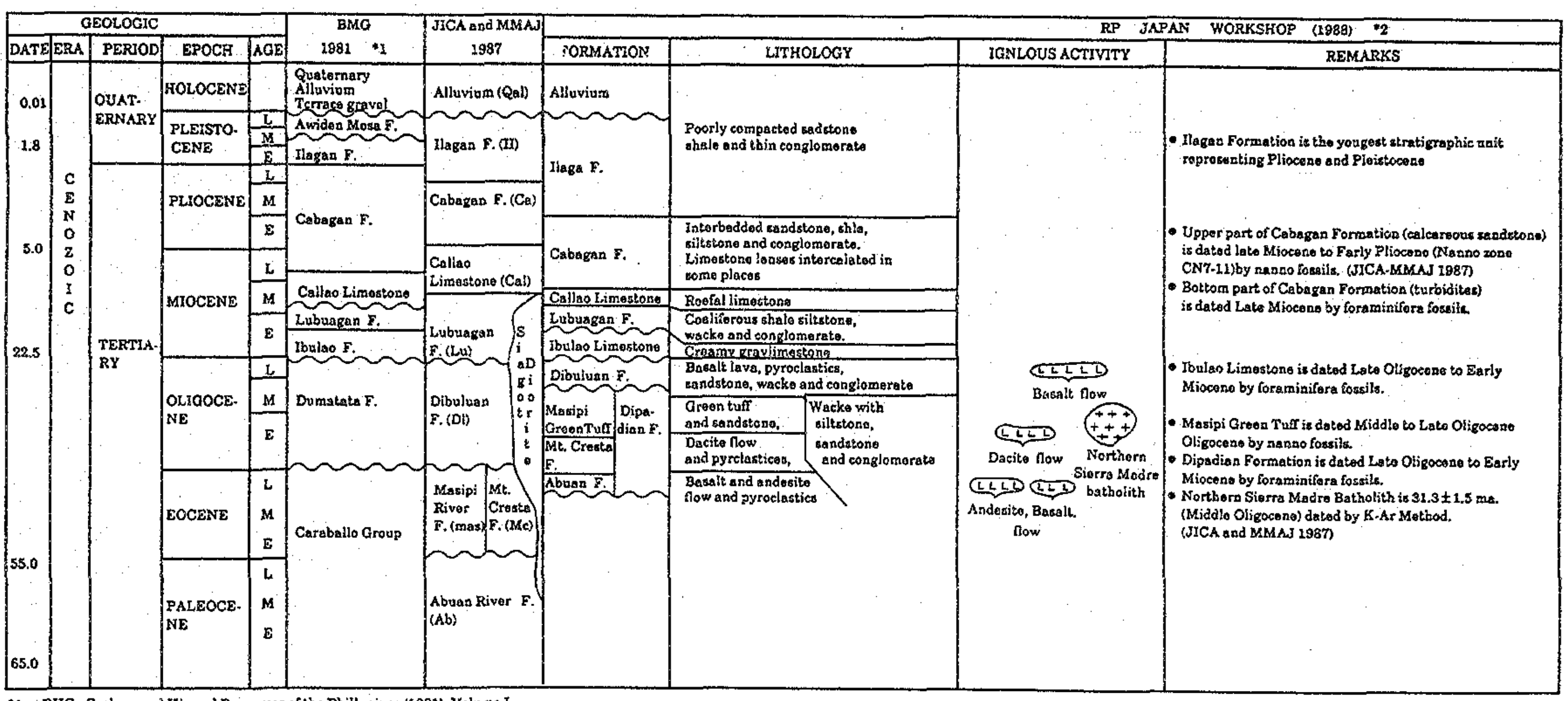

*1 BHG: Geology and Hineral Resources of the Phillupines (1981), Volume I p. 38 (Table II-13)
*2 M.A. Aurelio and E.B.Billedo. Tectonic Implicatiojn of the Geology and Minera Resources of Northern Sierra Hadre. ms. (1987)

Fig. 6 Stratigraphic Column of the Western Part of the Area

The lava flows are characterized by columnar joints while the pyroclastic sediments are sandy and show well-defined beddings.

The well-bedded Masipi Green Tuff conformably overlies the Mt. Cresta Formation.

The Masipi Green Tuff represents a sequence of parallel bedded greenish tuff, tuffaceous sandstone and some pyroclastics found at the type locality, Masipi River in Cabagan.

The nannofossils contained in tuffaceous sandstone indicate a Middle to Late Oligocene age. (JICA-MMAJ, 1987.)

The Abuan Formation, Mt. Cresta Formation and Masipi Green Tuff were deposited in an environment characterized by continuous sedimentation, and they are thought to have a contemporaneous heteropic facies relationship with the Dipadian Formation.

After the deposition of the Masipi Green Tuff, the Northern Sierra Madre Batholith intruded into the area.

The Dibuluan Formation consists of basaltic flows and pyroclastics and it unconformably overlies the Abuan Formation, Masipi Green Tuff and the Northern Sierra Madre Batholith. It embodies the principal position of the westward dipping monoclinal structure of the Cagayan Basin. It is thought to be of Late Oligocene age.

The Ibulao Limestone unconformably overlies both the Dibuluan Formation and the Masipi Green Tuff. It is characterized by well-bedded limestone with varing thicknesses and interbeds of calcarenites and calcirudites. The formation is assigned a Late Oligocene to Early Miocene age. It is exposed along the Dicamay River in the southern part of the area.

Exposure of this formation at the northern portion of the area has been noted to be accompanied intermittently by the Dibuluan Formation. It has also been observed around the vicinity of Cabagan.

The Lubuagan Formation consists coaly shale, coaliferous beds, sandstone and conglomerate and is estimated to be over 10,000 m in thickness. The lower part of the formation is characterized by rhythmically deposited layers of sandstone and shale of flysh-type sequence, and massive sandstone and graywacke. The middle part consists of well-bedded conglomerate while the upper part is made up mainly of sandstone which is believed to have been deposited in a shallow sea environment. These geologic characteristics, especially the existence of the cobble containing coglomerate with sandstone and siltstone intercalation suggest turbulent flow deposition. The upper part of this formation is referred to be the shallow water equivalents of turbidites (Aurelio and Billedo, 1987).

This formation trending NNW is distributed from the eastern part of Ilagan to the eastern part of Tuguegarao. This formation is deposited in Early to Middle Miocene.

The Callao Limestone possesses two distinct features. The lower part is massive, poorly bedded, cliff-forming, relatively resistant to weathering and represents the shelfal-type lime deposits. The upper part is a coralline reefal facies which is better bedded and less dense than the lower part.

This limestone body has been identified to be of Middle Miocene age. In general, the Callao Limestone was deposited within the paleo-environmental limits of the neritic and littoral zones. The lower part of this formation has intertongueing relationship with the upper part of the Lubuagan Formation. The upper part of this formation, on the other hand, has interbedded members of the Cabagan Formation. This formation is exposed in a crecent-like shape from Ilagan up to the northern foothills of Twin Peak.

The Cabagan Formation can be divided lithologically into three, namely, the Cabagan Turbidites in the bottom, the Cabagan Conglomerates in the middle and the Cabagan Calcarenites on top. The turbidites are well-bedded layers of alternating sandstones and shales. It is difficult to clearly distinguish this turbidite from the Lubuagan Turbidite by its appearance. The sandstones are usually medium to coarse-grained and sparsely fossiliferous while the shale layers are slightly calcareous with abundant fossils. The age of this turbidite is assumed to be Late Miocene (JICA-MMAJ, 1987). The Cabagan Conglomerates consists of a thick pile of cobble conglomerates, containing well-rounded clasts of altered andesite and spillites and reworked Late to Middle Miocene limestones, thought to belong to the Callao Limestone. The Cabagan Calcarenite, the upper part of this formation, is dominated by calcareous sandstones, shale and mudstone. This formation covers the Callao Formation conformably and is distributed widely from the southern part to the northern part of the project area. Nannoplankton determination gave an Early Pliocene age.

The Ilagan Formation is the uppermost sedimentary unit in the project area and covers nearly all of the Cagayan Basin. It is composed of bedded but poorly compacted sandstones, shales and thin polymictic conglomerates. The lower part of this formation is a shallow marine deposit. But toward the top, the rocks increase in clastic size into conglomerates made up mostly of pebbles and cobbles that exhibit imbricate structures. This characteristic implies deposition in a fluviatile environment. The Ilagan Formation covers the Cabagan Formation conformably and the deposition is thought to have occurred during Pliocene to Pleistocene.

2-1-3 Geologic Structure

The evolution of the geology and structures of the Northern Sierra Madre Area are intimately associated with the subduction events along its eastern coast. Subduction is believed to have begun in Eocene and had ceased in the Late Oligocene age and had been reactivated during the Holocene. The East Luzon Trough as it is today is actually an incipient subduction zone that has been superimposed on an old convergent margin (the old East Luzon Trough) leading to its apparent reactivation. This explains why inspite of the young age of the East Luzon Trough, it has characteristics that are only found in well-developed subduction zones (Lewis & Hayes, 1983., Hamburger et al., 1983).

Tectonic reconstruction had led to the recognition of a backarc basin along the west side of the Northern Sierra Madre Range. Post-Oligocene sediments which were deposited on this basin dip gently westward and define a monoclinic structure. A rift valley trending E-W has also been observed within the Paret Embayment area around Baggao which is in the northern part of the recognized backarc basin.

On the other hand, the San Mariano Embayment (syncline) is characterized by a basin around the Cagayan area in the southern part of the project area. Normal faults had been observed in areas between this basin and the mountain range. A N-S trending thrust is present along the east side of the mountain range. This thrust extends about 90 km from Dinapiqui Point to the Divilacan Bay of the eastern coast.

It divides the survey area into two terranes: One is the East Tectonic Terrane consisting of an ophiolite suite of Early Cretaceous age and the other is the Central Tectonic Terrane comprising formations and intrusives of post-Eocene age. The age for the cessation of activities of the Divilacan thrust is inferred to be Late Oligocene as it is unconformably overlain by the Dierico Formation of Early to Middle Miocene age.

The Divilacan Thrust has an important significance on the geologic structure of the survey area and therefore detailed survey and investigations are necessary.

The Eastern Part is mainly composed of a Cretaceous ophiolite basement. A NE-SW trending depression is also present in this area. Tertiary sedimentary formations were desposited on this depression.

The Isabela Ultramafic Complex, Bicobian Basalt and Dikinamaran Chert are in tectonic contact with each other. Thus, it is difficult to understand their original stratigraphic relationships. The geologic structure in the eastern part is very complicated.

2-1-4 Igneous activities

Igneous activities observed in the Northern Sierra Madre Area are as follows:

2-1-4-1 The igneous activities of the Eastern Part

Igneous activities of this area are believed to be related to oceanic crust formation leading to the formation of the Bicobian Basalt and other related lithologies.

2-1-4-2 The igneous activities of the Western Part

(A) Eocene to Early Oligocene Igneous activities:
During this period activity, the basaltic and andesitic flows and pyroclastic rocks of the Abuan Formation were formed followed by the dacitic flows of the Mt. Cresta Formation and lastly the Masipi Green tuff were deposited.

(B) The Northern Sierra Madre Batholith:
This large batholith occurs along the Northern Sierra Madre Range, elongated in N-S direction. This intruded into four Eocene to Early Oligocene formations namely, Dipadian Formation, Abuan Formation, Mt. Cresta Formation and Masipi Green Tuff and forms stocks or cupolas with the contact aureole best exemplified in the Mt. Cresta Formation. The composition varies from tonalite to quartz-diorite to granodiorite with variable amounts of ferro-magnesian minerals. The age of intrusion is determined to be Late Oligocene by K-Ar dating (22 to 31 Ma.).

(C) Late Oligocene igneous activity:
By this igneous activity, the basaltic flows and pyroclastics which compose the principal part of the DibuluanFormation were formed. After this event, no igneous activity is known in the Northern Sierra Madre Area.

2-2 Mineralization

Four principal types of mineralization have been observed in this area as follows:

The mineral showings investigated in the survey area are shown in Tables-1 and -2.

2-2-1 Orthomagmatic mineralization

The Ni and Cr concentration occurred during the process of the magmatic differenciation of the Isabela Ultramafic Complex.

This type of mineralization is found in the ophiolite of the Eastern part of the area. e.g. Cas Chrome Wasayan II (35*), Dibenelang (43*), etc. (*: numbers correspond to mineral showing number in Table-1 and -2.)

2-2-2 Cyprus type, massive sulphide copper mineralization

It occurs along the upper boundary of the Bicobian Basalt and Dikinamaran Chert.

These types of mineral showings occur associated with the Bicobian Basalt in the ophiolite zone along the east coast. Typical mineral showing of this type can be found at Bicobian to the west of Port Bicobian.

2-2-3 Sulfide dissemination in volcanic breccias associated with Oligocene basalt

This type of mineralization is observed within volcanic breccias associated with the basalt of the Abuan Formation at the southeastern part of the Northern Sierra Madre Range. Typical mineral showing of this type is the Dimakawal mineral showing. This showing is hydrothermal fissure filling veins of copper sulfide. The mineralization occurs in a hydrothermal alteration zone with the associated veins and veinlets controlled by a system of fractures, and associated dissemination of copper sulfides. The dominant hydrothermal alterations are silicification and chloritization (Cabantog,unpub. 1973).

2-2-4 Porphyry copper type mineralization

This mineralization occurs along the contact between the dacitic (Mt. Cresta Formation) to andesitic (Abuan Formation) rocks and the diorite bodies (Northern Sierra Madre Batholith).

Typical mineral showing of this type is Casablangan (14*) which is located at the northern part of the Northern Sierra Madre Range.

The only operating mine in the Northern Sierra Madre area is the Wasayan (I) mine (Cas Chrome Corp., Co.). The ore deposit of this mine is the orthomagmatic chromite type, associated with the Ophiolite of the Eastern Part. The ore shoots occur in lenticular dunite and the widths vary widely.

The mine at present is mining the chromite floats in the laterite zone. The mine has been shipping chromite ore since 1983 totaling to about 15,000 tons of concentrates (grade 43% Cr_2O_3). Production rate of concentrates per month is around 400 t.

Table-1 Major Mineral Showings in the Eastern Part

MINERAL SHOWING *1 NAME	LOCATION	COMMODITY AND MENERALIZATION	AGE *2	TECTONIC PROVINCE	DESCRIPTION	
					OCCURENCE	CHEMICAL ASSY OF SAMPLE
9 Dikadiaoan	122°27' E 17°00' N	Mn strata-bound	Cretaceous	Oceanic crust	Manganese wad with manganiferous chert	Banded sample of manganese wad & chert; SiO_2 47.94%, MnO 4.80%, Fe 20.66%
17 Disawit	122°29' E 16°59' N	Mn strata-bound	Cretaceous	Oceanic crust	Strata-bound manganese in basalt flow and chert	Banded sample of manganese wad & chart; SiO_2 45.28%, MnO 4.86%, Fe 19.81%
26 Kanaipang Hill	122°27' E 16°58' N	Mn strata-bound	Cretaceous	Oceanic crust	Strata-bound manganese in tuffaceous sediments	Boulder of manganiferous sediment; SiO_2 50.26%, Mn 6.77%, Fe 18.44%, P 0.2%, CaO 0.62%
28 Bicobian	122°24' E 17°15' N	Cu strata-bound massive sulfide	Cretaceous	Oceanic crust	Cyprus type massive sulfide in footwall of pillow basalt	*3 Massive sulfide boulder; Au 5.5g/t, Ag 168.5g/t, Cu 54.4%, Zn 0.26%, S 26.14%, (bearing chalcocite)
34 Cas Chrome Wasayan I	122°17' E 16°35' N	Cr ortho magmatic	Cretaceous	Oceanic crust	Operating mine	
35 Cas Chrome Wasayan II	122°18' E 16°35' N	Cr ortho magmatic	Cretaceous	Oceanic crust	Disseminated chromite in lateritized dunite	Lenticular chromite; Cr_2O_3 53.39%, Al_2O_3 14.95%, FeO 14.50%, SiO_2 0.40%, MgO 13.11%
39 Dikapisan	122°27' E 16°53' N	Cr ortho magmatic	Cretaceous	Oceanic crust	Chromite lens in dunite	
43 Dibenelang	122°20' 24" E 17°17' 42" N	Cr ortho magmatic	Cretaceous	Oceanic crust	Massive chromite in dunite	Massive chromite; Cr_2O_3 46.35%, Al_2O_3 10.91%, FeO 13.32% SiO_2 6.79%, MgO 17.53%
44 Lacson	122°23' 04" E 17°14' 33" N	Cu strata-bound massive sulfide	Cretaceous	Oceanic crust	Cyprus type massive sulfide at top of altered pillow basalt	Masive sulfide; Au 0.5g/t, Ag 12.1g/t, Cu 7.46%, Zn 0.26%, S 46.67%
46 Disukad	122°23' 06" E 17°11' 15" N	Cr ortho magmatic	Cretaceous	Oceanic crust	Blocks of disseminated chromite in lateritized dunite	
47 Dilacnadinom	122°19' 40" E 17°11' 05" N	Cr ortho magmatic	Cretaceous	Oceanic crust	Composite layers of chromite in serpentinized dunite and peridotite	

*1 Numbers; corresponds to those in Plate-7.
*2 Chromite, manganese and massive sulfide bodies associated with Cretaceous ophilolite which emplaced along east Luzon Fore Arc during Oligocene.
*3 This sample is composed mainly of secondary chalcocite, therefore does not represent the average grade.

Table-2 Major Mineral Showings in the Western Part

MINERAL SHOWING *1 NAME	LOCATION	COMMODITY AND MINERALIZATION	AGE	TECTONIC PROVINCE	DESCRIPTION	
					OCCURENCE	CHEMICAL ASSAY OF SAMPLE
6 Menuma	122°05' E 07°06' N	Cu Porphyry copper	Oligocene to Miocene	Volcanic and plutonic arc	Pyrite dissemination in marginal part of diorite stock	Altered rock sample; Cu 0.01%, Zn 0.04%, Fe 2.94%
7 Siagot	122°04' E 17°06' N	Cu Dissemination	Oligocene to Miocene	Volcanic and plutonic arc	Pyrite dissemination in silicified diorite	Silicified rock sample; Cu 0.001%, Zn 0.002%, Fe 2.71%
8 Ilagan	122°04' E 17°08' N	Cu Dissemination	Oligocene to Miocene	Volcanic and plutonic arc	Pyrite dissemination in quartz diorite	Altered diorite sample; Cu 0.006%, Zn 0.011%, Fe 5.71%
11 Isabela	122°05' E 17°09' N	Cu Porphyry copper	Oligocene to Miocene	Volcanic and plutonic arc	Pyrite dissemination in altered zone around diorite stock	Altered diorite sample; Cu 0.001%, Zn 0.009%, Fe 4.89%
⑭ Casablangan	122°00' E 17°37' N	Cu Porphyry copper	Oligocene to Miocene	Volcanic and plutonic arc	Pyrite, chalcopyrite dissemination in dacite	Pyrite disseminated sample; Cu 0.027%, Zn 0.009%, Fe 6.68%, Ag 21g/t
⑮ Dinacdacan	122°02' E 17°34' N	Cu Porphyry copper	Oligocene to Miocene	Volcanic and plutonic arc	Pyrite, chalcopyrite dissemination in dacite	Pyrite disseminated sample; Cu 0.007%, Zn 0.08%, Fe 1.29%, Ag 8g/t
⑯ Capisayan West	121°54' E 18°03' N	Fe Sedimentary	Pliocene	Back arc basin	Sedimentary sequence in pliocene formation	Magnetite rich layer sample; Ag 26g/t, Cu 0.017%, Zn 0.015%, Fe 13.26%
⑰ Capisayan East	121°55' E 18°03' N	Fe Sedimentary	Pliocene	Back arc basin	Sedimentary sequence in pliocene formation	Outcrop; length 150m thickness 0.5m
19 Dimakawal	122°12' E 16°35' N	Mn Strata-bound Cu Dissemination	Oligocene to Miocene	Volcanic and plutonic arc	Strata-bound manganese and sulfide dissemination in volcanic breccia	Manganese sample; SiO_2 13.97%, Mn 45.47%, Fe 8.49%, P 0.05%, CaO 1.72% Sulfide sample; Au 0.1g/t, Ag 132.3g/t, Cu 15.88%, Zn 23.00%, S 18.5%
37 Dinapiqui	122°13' E 16°36' N	Cu, Au Vein	Oligocene to Miocene	Volcanic and plutonic arc	Pyrite, chalcopyrite mineralization in basalt	Quartz vein (w: 20cm) sample; Au 0.1g/t, Ag 4.5g/t, Cu 0.23% S 2.87%, Fe 2.23%
38 Dimatatno	122°15' E 16°39' N	Cu Vein	Oligocene to Miocene	Volcanic and plutonic arc	Quartz vein in andesite	Quartz vein sample (w: 0.15m); Au tr, Ag tr, Cu 0.02%, Fe 4.27%
41 Giwed	122°21' E 16°56' N	Cu Dissemination and vein	Oligocene to Miocene	Volcanic and plutonic arc	Quartz vein in andesite	Silicified zone sample; Au tr, Ag tr, Cu 0.01%, S 1.34%, Fe 4.37%
42 Diudenan	122°21' E 16°57' N	Cu Vein	Oligocene to Miocene	Volcanic and plutonic arc	Quartz vein in andesite	Quartz vein sample (w: 0.4m); Au tr, Ag tr, Cu 0.01%, Fe 1.50%
45 Bolos River	122°08' E 17°25' N	Cu Vein	Oligocene to Miocene	Volcanic and plutonic arc	Calcite vein associated sheared zone in diorite	Sheared zone sample (w: 2m); Au tr, Ag tr, Cu 0.01%, Fe 4.08%
48 Disdo Creek	122°01' E 16°34' N	Au Quartz vein	Oligocene to Miocene	Volcanic and plutonic arc	Quartz vein in meta-andesite	Quartz vein sample; Au 0.07g/t, Ag 1.7g/t, Cu 0.03%
49 Dina Creek	122°13' E 16°49' N	Cu, Au Vein	Oligocene to Miocene	Volcanic and plutonic arc	Veinlets, dissemination in meta-andesite near diorite stock	Sheared chloritized andesite; Au 0.14g/t, Ag 9g/t, Cu 3.07%
50 Diwagao	122°12' E 16°41' N	Au, Cu Unknown	Unknown	Volcanic and plutonic arc	Only float sample available	Float sample; Au 2.5g/t, Ag 0.07g/t, Cu 0.07%
51 Dicamay River	121°54' E 16°31' N	Fe? Unknown	Uknown	Volcanic and plutonic arc	Only float sample available hematite in calcareous conglomerate	
52 Ilagan River	122°03' E 16°38' N	Au Network dissemination	Oligocene to Miocene	Volcanic and plutonic arc	Pyrite dissemination in altered zone around diorite stock	Altered zone sample; Au<0.07g/t, Ag 0.3g/t, Cu<0.01%
53 Diden River	122°04' E 16°37' N	Au? Ag? Network	Oligocene to Miocene	Volcanic and plutonic arc	Pyrite dissemination in altered andesite around diorite stock	Altered andesite sample; Au<0.07g/t, Ag 1.7g/t, Cu<0.01%
54 Palig Creek	122°11' E 16°37' N	Cu?, Au? Vein type	Oligocene to Miocene	Volcanic and plutonic arc	Quartz, pyrite veins in argillized andesite near diorite stock	

*1 Numbers; correspond to those in Plate-7.

3. Geochemical Sample Analyses and Data Processing

3-1 Analytical Methods and Precision

3-1-1 Analytical Methods

The survey area where 4,973 stream sediment samples were collected is divided into 2,180 cells (2km × 2km) based on the datum point (121° 30' east longitude, 16° 30' north latitude.). The geometric average of results of analyses of each cell is calculated.

The four kinds of statistical analyses method were conducted on these cell average values. These methods are as follows:

(A) Univariate analyses of the geometrical average values of the results of chemical analyses of each cell.
(hereinafter called cell average value).

(B) Univariate analyses of the moving average value which the average value of nine cells is estimated to be the value of the central cell.

(C) Univariate analyses of the high-pass filter value which is the positive difference when the moving average value is deducted from the cell average value.

(D) Multivariate analyses (Factor Analyses) for cell average value.

3-1-2 Chemical Analysis

A total of 4,973 stream sediment samples were collected in the Northern Sierra Madre Area (grain size less than 0.175 mm). These samples were sent to PETROLAB, one of the MGB sections in charge of chemical analysis. Microchemical analyses were carried out by atomic absorption spectroscopy (AAS).

The 11 elements analysed are as follows; Cu, Pb, Zn, Ag, As, Mn, Ni, Co, Mo, Hg and Cr.

Analytical flow charts are shown in Appendices Figures 2-1 to 2-4.

The average of the number of samples is 2.28 per each cell.

An IBM3084Q computer and statistical analyses package BMD 08M (UCLA developed) were utilized on statistical procedures. All geochemical values inputted into the computer utilized logarithmic values with the results being converted in to normal value. For the purpose of the statistical procedure, the 50% values of the detection limit were given the cells which have the geometric average value below the detection limit.

Detection limits of AAS analyses in PETROLAB are estimated as follows.

Table-3 Detection Limits of AAS Analyses (ppm)

Element	Cu	Pb	Zn	Ag	As	Mn	Ni	Co	Mo	Hg	Cr
Detection limit value	2	10	2	1	0.5	50	3	3	2	0.04	100

As for Ag, the cells which showed the cell average values over the detection limit value were only two, thus Ag was omitted from these statistical analysis.

3-1-3 Precision Check

Precision checks for the chemical analyses were carried out. The variance of analyzed value at 95% confidence level is calculated by the Thompson and Howarth method (1973).

Batch test results.

A) Process of the batch test
A sample is chosen from each analyzed batch (about 20 samples) and is analyzed with another batch, after which the variance is calculated by the statistically.

B) Results of precision check

Table-4 Dispersion of Batch Test Results

Element	Variance	Remark
Cu	±15%	The variance of Ag and Mo can not be determined because the contents in many samples were below detection limit.
Pb	±20%	
Zn	±20%	
As	±25%	
Mn	±10%	
Ni	±20%	
Co	±20%	
Hg	±25%	
Cr	±30%	

3-2 Data processing

3-2-1 Univariate analyses

3-2-1-1 Cell average values

As mentioned above, the average number of samples is 2.28 per each cell. For blank cell which has no sampling point, gap filling is done as follows.

Geometrical average value of the 8 cells around the blank cell is applied as the value of the blank cell. When the effective values are less than 4 cells, gap filling is not done. This gap filling procedure was done twice.

3-2-1-1-1 Basic statistical values

The basic statistical values of the cell average values for each element are shown on Table-5, and the basic statistical values of the original analytical results are shown in Table-6 for reference.

Table-5 Basic Statistical Values for the Cell Average Values

	Cu (ppm)	Pb (ppm)	Zn (ppm)	Ag (ppm)	As (ppm)	Mn (ppm)	Ni (ppm)	Co (ppm)	Mo (ppm)	Hg (ppb)	Cr (ppm)
$\overline{X}$	41.00	5.11	88.22	0.50	1.73	1,083.58	32.64	27.14	1.03	21.07	340.75
$\overline{X}+1.0\sigma$	65.18	6.02	136.21	0.52	4.24	1,641.63	137.31	48.65	1.20	25.65	2,232.62
$\overline{X}+1.5\sigma$	82.21	6.32	169.25	0.53	6.63	2,020.60	281.64	65.15	1.30	28.26	5,719.81
$\overline{X}+2.0\sigma$	103.66	6.78	210.31	0.54	10.36	2,487.06	577.67	87.23	1.40	31.16	14,628.13
Minimum	6.67	5.00	13.00	0.50	0.25	290.00	3.00	4.00	1.00	20.00	50.00
Maximum	518.80	66.50	1,565.40	2.00	115.92	33,575.00	6,100.00	461.00	15.00	190.00	149,000.00
Number of cell	2,180	2,180	2,180	1,539	2,180	2,180	2,180	2,180	2,180	2,180	2,177
R.B.D.	0%	98.9%	0%	99.9%	8.3%	0%	0%	0%	98.7%	97.3%	30.7%

$\overline{X}$: Mean value σ : Standard deviation R.B.D. : Ratio of below detection limit value

Table-6 Basic Statistical Values of the Original Analyses

	Cu (ppm)	Pb (ppm)	Zn (ppm)	Ag (ppm)	As (ppm)	Mn (ppm)	Ni (ppm)	Co (ppm)	Mo (ppm)	Hg (ppb)	Cr (ppm)
$\overline{X}$	39.78	5.07	84.99	0.50	1.61	1,040.46	30.40	25.73	1.02	20.86	283.15
$\overline{X}+1.0\sigma$	70.21	5.93	141.76	0.53	4.56	1,705.31	129.56	48.57	1.23	26.16	1,920.30
$\overline{X}+1.5\sigma$	93.28	6.41	183.08	0.54	7.68	2,183.20	267.47	66.44	1.36	29.30	5,000.91
$\overline{X}+2.0\sigma$	132.92	6.93	236.45	0.55	12.92	2,795.00	552.19	91.70	1.49	32.81	13,023.49
Minimum	1.00	5.00	10.00	0.50	0.29	100.00	1.50	1.50	1.00	20.00	50.00
Maximum	1,040.00	110.00	3,400.00	4.00	210.00	50,000.00	6,200.00	530.00	24.00	460.00	161,000.00
Sample No.	4,973	4,973	4,973	3,581	4,973	4,973	4,973	4,973	4,973	4,973	4,930
R.B.D.	0%	98.9%	0%	99.9%	0%	0%	0%	0%	98.3%	96.0%	30.7%

$\overline{X}$: Mean value σ : Standard deviation R.B.D. : Ratio of below detection limit value

3-2-1-1-2 Histograms and cumulative frequency curves

Histograms and cumulative frequency curves are shown in the attached plates at the end of this volume (Attached data-1).

The ranges of anomalous values were determined from these data as follows.

Cu: Inflection point of the curve at the point 80% cumulative frequency which corresponds to $\overline{X}+1.0\sigma$ value (60 ppm) was used as the threshold value.

Pb: About 99% of the cells contained amounts below detection limit. The limit of anomalous values is therefore not clear.

Zn: Inflection point of the curve observed at the 95% point cumulative frequency which corresponds to $\overline{X}+1.5\sigma$ value (174 ppm) was used as the threshold value.

Ag: Over 99% of the cells contained amounts below detection limit. Thus the range of anomalous values is unclear.

As: The cumulative frequency curve shows inflection point at 97% which corresponds to $\overline{X}+1.5\sigma$ value (7 ppm). This value was used as the threshold value.

Mn: Inflection point of the curve observed at 92% cumulative frequency which corresponds to $\overline{X}+1.0\sigma$ value (1,700 ppm). This value was used as the threshold value.

Ni: The cumulative frequency curve shows inflection point at 88% cumulative frequency which corresponds to the values between $\overline{X}+1.0\sigma$ value and $\overline{X}+1.5\sigma$ value (200 ppm). This value was used as the threshold value.

Co: The curve shows inflection point at 95% cumulative frequency which corresponds to $\overline{X}+1.5\sigma$ value (70 ppm). This value was used as the threshold value.

Mo: About 98% of the cells contain amounts below detection limit. Thus the range of the anomalous values is unclear.

Hg: About 97% of the cells contain amounts below detection limit but, thus the curve was out of logarithmic normal dispersion.

Cr: The curve shows inflection point at 90% cumulative frequency and it corresponds to values between $\overline{X}+1.5\sigma$ and $\overline{X}+2.0\sigma$ (9,000 ppm). This value was used as the threshold value.

3-2-1-1-3 Correlation coefficients among elements

Correlation coefficients among elements are shown in Table-7, Table-8.

Table-7 Correlation Coefficients in Cell Average Value

	Cu	Pb	Zn	Ag	As	Mn	Ni	Co	Mo	Hg	Cr
Cu	1.000										
Pb	0.198	1.000									
Zn	0.562	0.296	1.000								
Ag	0.094	0.531	0.086	1.000							
As	0.165	0.262	0.191	0.112	1.000						
Mn	0.398	0.260	0.633	0.177	0.187	1.000					
Ni	0.115	− 0.034	0.041	0.030	− 0.003	0.240	1.000				
Co	0.242	− 0.083	0.216	− 0.034	− 0.037	0.487	0.827	1.000			
Mo	− 0.008	0.153	− 0.014	− 0.008	0.182	− 0.122	− 0.067	− 0.070	1.000		
Hg	0.114	0.379	0.132	0.391	0.146	0.286	0.267	0.237	0.013	1.000	
Cr	− 0.029	− 0.056	0.012	− 0.015	0.030	0.168	0.888	0.716	− 0.066	0.197	1.000

Table-8 Correlation Coefficients of the Original Analyses

	Cu	Pb	Zn	Ag	As	Mn	Ni	Co	Mo	Hg	Cr
Cu	1.000										
Pb	0.184	1.000									
Zn	0.537	0.276	1.000								
Ag	0.056	0.327	0.072	1.000							
As	0.232	0.207	0.196	0.080	1.000						
Mn	0.408	0.236	0.638	0.139	0.187	1.000					
Ni	0.146	− 0.023	0.050	0.025	− 0.002	0.232	1.000				
Co	0.317	− 0.059	0.245	− 0.020	− 0.026	0.478	0.795	1.000			
Mo	− 0.010	0.076	− 0.038	− 0.005	0.135	− 0.139	− 0.049	− 0.035	1.000		
Hg	0.128	0.358	0.132	0.213	0.123	0.237	0.190	0.178	0.022	1.000	
Cr	− 0.013	− 0.043	0.027	− 0.003	− 0.003	0.161	0.862	0.864	− 0.051	0.128	1.000

In the cell average values positive correlations are observed among the following elements.

Cu-Zn, Pb-Ag, Zn-Mn, Ni-Cr, Co-Cr.
\
Co

3-2-1-1-4 Areal distribution of the cell average values. (Attached plate 2-1 No. 1-No. 10)

The cell average values of each element are classified into 11 ranks and plotted in a 1:1,000,000 scale areal map with corresponding rank colors.

Classified ranges are as follows.

Code	Cumulative frequency range
A	99% ≦ Z
B	95% ≦ Z < 99%
C	90% ≦ Z < 95%
D	75% ≦ Z < 90%
E	60% ≦ Z < 75%
F	50% ≦ Z < 60%
G	40% ≦ Z < 50%
H	30% ≦ Z < 40%
I	20% ≦ Z < 30%
J	Detection Limit ≦ Z < 20%
K	Detection Limit > Z

The areal distribution zone of the anomalous cell average values of each element are as follows.

North side of Capisayan in the northern part of the survey area. (Anomalous elements; Cu, Zn and Mn)

West side of Awang Cove in the northern part of the east coast. (Anomalous elements; Cu and Mn)

Upstream section of Tuguegarao River in the central mountain range. (Anomalous elements; Cu, Zn and As)

South side of Divilacan Bay in the central east coast. (Anomalous elements; Cu, Zn, Mn, Ni, Co, Hg and Cr)

West side of Port Bicobian in the central east coast. (Anomalous elements; Cu, Mn, Ni, Co, Hg and Cr)

West side of Digollorin Point to Dinatadmo Point in the east coast. (Anomalous elements; Ni, Co, Hg and Cr)

Vicinity of the Dimakawal mineral showing in the southeastern part of the area. (Anomalous elements; Cu, Pb, Zn, Mn and Hg)

Of the above, the anomalies of the following six zones can be understood by the present knowledge regarding the respective geological settings, igneous activities and mineralization. The numbers of the zones below correspond to that of the above listing.

(a) North side of Capisayan in the northern part of the survey area: Late Miocene to Early Pliocene Cabagan Formation is distributed in this zone and stratified iron mineral showings are known.

(b) Upstream of Tuguegarao River in the central mountain range; Diorite stocks which belong to the Northern Sierra Madre Batholith were intruded in this zone.
Porphyry copper mineralization is assumed on the basis of the assemblage of anomalous elements.

(c) South side of Divilacan Bay in the central east coast: The Isabela Ultramafic rocks, Bicobian Basalt and Dikinamaran Chert are distributed in this zone. The Divilacan thrust which divides the survey area into two tectonic terraanes passes through the west side of this zone. Ni, Co and Cr anomalous values are related to the ultramafic rocks.

(d) West side of Port Bicobian in the central east coast; Cretaceous Dikinamaran Chert, Bicobian Basalt, etc. are exposed in this zone. Cyprus type massive sulfide showings and stratified manganese showings are known.

(e) West side of Dinatadmo Point in the southern part of the east coast; The Isabela Ultramafic rocks are distributed in this zone, Ni, Co and Cr anomalous values are probably derived from these ultramafic rocks. Cas Chrome Wasayan I, the only operating mine in the eastern Part is located in this zone.

(f) Vinicinity of the Dimakawal mineral showing in the southeastern part of the area: The Early Oligocene Abuan Formation and diorite stocks belonging to the Northern Sierra Madre batholith are exposed in this zone. Several massive sulfide and vein type mineral showings are known. Polymetallic anomalous values are assumed to have been derived from these mineralization.

3-2-1-2 Moving average values

Moving average values were carried out by the procedure stated in 3-1-1.

The gap filling procedure for a blank cell at the edge is done in such a way that when there are effective values in 3 cells among the five cells which enclose the blank cell as embayed shape, the average value of these three values is taken as the moving average value of the embayed blank cell.

The blank cells were filled by a set procedure twice.

These anomalous zones are shown in a large scale than the cell average values, as a result of smoothing.

3-2-1-2-1 Basic statistical values

Moving average procedure was applied to 2,180 cell average values and the basic statistical values were calculated. Details are shown in Table-9.

3-2-1-2-2 Histograms and cumulative frequency curves

Histograms and cumulative frequency curves which show dispersion of the moving average values are presented separately for each element.

The range of anomalous values were determined from these data.

The anomalous ranges of each element are as follows:

Cu: The curve shows the inflection point at 92% cumulative frequency which corresponds to the $\overline{X}+1.5\sigma$ value (70 ppm). This value was used as the threshold value.

Pb: The contents in 99.7% cells show below detection limit values. The range of anomalous values is, therefore, not clear.

Zn: The curve shows inflection point at 90% cumulative frequency which corresponds to the value between $\overline{X}+1.0\sigma$ and $\overline{X}+1.5\sigma$ value (134 ppm). This value was used as the threshold value.

Ag: All cells contain amounts below detection limits, thus Ag values were omitted from the statistical analysis.

As: The curve shows inflection point at 90% cumulative frequency which corresponds to the value between $\overline{X}+1.0\sigma$ and $\overline{X}+1.5\sigma$ value (4.6 ppm). This value was used as the threshold value.

Mn: The curve shows inflection point at 90% cumulative frequency which corresponds to the value between $\overline{X}+1.0\sigma$ and $\overline{X}+1.5\sigma$ value (1,590 ppm). This value is used as the threshold value.

Ni: The curve shows inflection point at 90% cumulative frequency which corresponds to the value between $\overline{X}+1.5\sigma$ and $\overline{X}+2.0\sigma$ value (300 ppm). This value was used as the threshold value.

Co: The curve shows inflection point at 90% cumulative frequency which corresponds to $\overline{X}+1.0\sigma$ value (45 ppm). This value was used as the threshold value,.

Mo: About 99.7% of the cells contained amounts below detection limit. The anomalous range is therefore unclear.

Hg: About 99% of the cells contained amounts below detection limit value. The anomalous range is therefore unclear.

Cr: The curve shows inflection point at 90% cumulative frequency which corresponds to the value between $\overline{X}+1.5$ and $\overline{X}+2.0$ value (7,900 ppm). This value was used as the threshold value.

3-2-1-2-3 Areal distribution of the moving average values (Attached plate 2-2 No. 1-No. 10)

The moving average values of each element are classified into 11 ranks and plotted on a 1:1,000,000 scale areal map with each corresponding rank colors.

Classified ranges are as follows.

Code	Cumulative frequency range
A	99% ≦ Z
B	95% ≦ Z < 99%
C	90% ≦ Z < 95%
D	75% ≦ Z < 90%
E	60% ≦ Z < 75%
F	50% ≦ Z < 60%
G	40% ≦ Z < 50%
H	30% ≦ Z < 40%
I	20% ≦ Z < 30%
J	Detection Limit ≦ Z < 20%
K	Detection Limit > Z

The anomalous zones of each element are as follows. These coincide with the anomalous zones of cell average values. But concentration of anomalous cells is clearer than that of the cell average.

North side of Capisayan in the northern part of the survey area. (Anomalous elements; Cu, Zn and Mn)

Table-9 Basic Statistical Values of Moving Average Values

	Cu (ppm)	Pb (ppm)	Zn (ppm)	Ag (ppm)	As (ppm)	Mn (ppm)	Ni (ppm)	Co (ppm)	Mo (ppm)	Hg (ppb)	Cr (ppm)
$\overline{X}$	40.96	5.11	88.21	0.50	1.73	1,081.32	32.38	27.01	1.03	21.07	338.34
$\overline{X}+1.0\sigma$	59.84	5.56	124.46	0.51	3.62	1,499.79	124.35	45.49	1.12	24.00	1,897.42
$\overline{X}+1.5\sigma$	72.33	5.81	147.84	0.51	5.25	1,766.32	243.68	59.03	1.17	26.86	4,493.33
$\overline{X}+2.0\sigma$	87.42	6.06	175.61	0.52	7.59	2,080.21	477.52	76.60	1.22	28.67	10,640.74
Minimum	14.88	5.00	30.77	0.50	0.25	403.60	5.65	6.30	1.00	20.00	50.00
Maximum	164.99	17.56	376.49	0.70	19.48	8,839.89	3,293.65	244.92	2.58	61.29	84,140.78
Number of cell	2,205	2,205	2,205	1,552	2,205	2,205	2,205	2,205	2,205	2,205	2,200
R.B.D.	0%	99.7%	0%	100%	4.4%	0%	0%	0%	99.7%	98.9%	29.7%

$\overline{X}$: Mean value σ : Standard deviation R.B.D. : Ratio of below detection limit value

West side of Awang Cove in the northern part of the east coast. (Anomalous elements; Cu and Mn)

Upstream section of Tuguegarao River in central mountain range. (Anomalous elements; Cu, Zn and As)

South side of Divilacan Bay in the central east coast. (Anomalous elements; Cu, Zn, Mn, Ni, Co, and Cr)

West side of Port Bicobian in the central east coast. (Anomalous elements; Cu, Zn, Mn, Ni, Co and Cr)

Digollorin Point to Dinatadmo Point in the east coast. (Anomalous elements; Ni, Co and Cr)

Vicinity of the Dimakawal mineral showing in the southeastern part of the area. (Anomalous elements; Cu, Zn, As and Mn)

Of the above, the anomalies of the following six zones can be understood by their respective geological settings, igneous activities and mineralization as in the case of cell average anomalies.

(a) North side of Capisayan in the northern part of the survey area. The anomalous elements are same to that of cell average value. Late Miocene to Early Pliocene Cabagan Formation is distributed in this zone and stratified iron mineral showings are known.

(b) Upstream part of Tuguegarao River zone. The anomalous elements are same to that of average values. Diorite stocks which belong to the Northern Sierra Madre Batholith were intruded in this zone. Porphyry copper mineralization is assumed on the basis of the assemblage of anomalous element.

(c) South side of Divilacan Bay in the central east coast. Concentration of A, B and C rank cells are clearer than the cell average values.

(d) West side of Port Bicobian in the central east coast. Concentrations of A, B and C cells of anomalous elements are clearer than the cell average values. As compare with the cell average values, Hg anomalous cells are missing from this zone.

(e) West side of Dinatadmo Point in the southern part of the east coast. Concentration of A, B and C rank cells of anomalous elements are clearer than the cell average values. As compare with the cell average values, Hg znomalous cells are missing from this zone.

(f) Vicinity of the Dimakawal mineral showing in the southeastern part of the area. Concentration of A, B and C cells of anomalous elements are more clearer than the cell average values. As compare with the cell average values, as anomalous cells are containing to and Pb anomalous cells are missing from this zone.

3-2-1-3 High pass filter values

High pass filter values are the positive differences between the moving average values and the cell average values as mentioned in 3-1-1.

The deduction procedure aims to correct the local back-ground values which are indicated by the moving average values. Therefore, high-pass filter value indicates directly the anomalous zones which were derived from latter added factors such as mineralization, secondary enrichment and others, and provides guideline to the locality, strength and priority of the geochemical anomalous zones.

3-2-1-3-1 Basic statistical values

Basic statistical values are calculated from the cell average values and moving average values of each element, the details of which are shown in Table-10.

3-2-1-3-2 Histograms and cumulative frequency curves

Histograms and cumulative freqvency curves which show dispersion of the high-pass filter values are presented separately for each element.

The range of anomalous values were determined from these data.

The anomalous ranges of each element are as follows.

Cu: The curve shows inflection point at 79% cumulative frequency which corresponds to $\overline{X}+1.0\sigma$ value (16 ppm). This value was used as the threshold value.

Pb: The curve shows inflection point at 76% cumulative frequency which corresponds to $\overline{X}+1.0\sigma$ value (5 ppm). This value was used as the threshold value.

Zn: The curve shows inflection point at 79% cumulative frequency which corresponds to $\overline{X}+1.0\sigma$ value (36 ppm). This value was used as the threshold value.

Table-10 Basic Statistical Values of High-pass Filter Values

	Cu (ppm)	Pb (ppm)	Zn (ppm)	Ag (ppm)	As (ppm)	Mn (ppm)	Ni (ppm)	Co (ppm)	Mo (ppm)	Hg (ppb)	Cr (ppm)
$\overline{X}$	3.22	0.63	7.06	0.06	0.31	80.62	3.47	1.99	0.13	1.71	98.60
$\overline{X}+1.0\sigma$	16.14	4.96	35.76	0.69	1.78	377.14	44.18	10.00	1.17	15.05	1,616.07
$\overline{X}+1.5\sigma$	36.14	13.88	80.50	2.33	4.24	815.69	157.63	22.40	3.46	44.63	6,542.59
$\overline{X}+2.0\sigma$	80.94	38.84	181.23	7.91	10.09	1,764.24	562.40	50.16	10.25	132.35	26,487.39
Minimum	0.00	0.01	0.00	0.01	0.00	0.10	0.00	0.01	0.00	0.02	0.04
Maximum	418.40	54.87	1,199.81	1.30	109.75	30,530.01	4,779.26	318.86	12.42	136.41	99,698.08
Number of cell	1,016	78	1,002	5	1,050	1,016	1,011	1,023	91	210	997

$\overline{X}$: Mean value σ : Standard deviation

Ag: Effective high-pass filter value has existed only one, therefore Ag values were put off the analysis.

As: The curve shows inflection point at 79% cumulative frequency which corresponds to $\bar{X}+1.0\sigma$ value (1.8 ppm). This value was used as the threshold value.

Mn: The curve shows inflection point at 79% cumulative frequency which corresponds to $\bar{X}+1.0\sigma$ value (380 ppm). This value was used as the threshold value.

Ni: The curve shows inflection point at 91% cumulative frequency which corresponds to $\bar{X}+2.0\sigma$ value (550 ppm). This value is used as the threshold value.

Co: The curve shows inflection point at 92% cumulative frequency which corresponds to $\bar{X}+1.0\sigma$ value (10 ppm). This value was used as the threshold value.

Mo: The curve shows inflection point at 74% cumulative frequency which corresponds to $\bar{X}+1.0\sigma$ value (1.2 ppm). This value was used as the threshold value.

Hg: The curve shows inflection point at 74% cumulative frequency which corresponds to $\bar{X}+1.0\sigma$ value (1.5 ppb). This value was used as the threshold value.

Cr: The curve shows inflection point at 86% cumulative frequency which corresponds to $\bar{X}+1.5\sigma$ value (6,400 ppm). This value was used as the threshold value.

3-2-1-3-3 Areal distribution of high-pass filter anomalous values. (Attached plate 2-3 No. 1-No. 10)

Each anomalous value is classified based on the following formula, with each element plotted on a 1:1,000,000 map with the corresponding different color-red, yellow and blue.

Table-11 High-pass Filter Value Classification Formula

Rank	Classification formula	Color
A	$\bar{X}+2.0\sigma \leqq Z$	Red
B	$\bar{X}+1.5\sigma \leqq Z < \bar{X}+2.0\sigma$	Yellow
C	$\bar{X}+1.0\sigma \leqq Z < \bar{X}+1.5\sigma$	Blue

The anomalous zones which are strongly related to the high rank cells of the cell average value are essentially the same as those delineated by cell average.

The zones are listed below:

North side of Capisayan in the northern part of the area; (Anomalous elements; Cu, Zn and Mn)

West side of Awang Cove in the northern part of the east coast; (Anomalous elements; Cu, As and Mn)

Upstream of Tuguegarao River in the central mountain range; (Anomalous elements; Pb, Zn and As)

South side of Divilacan Bay in the central east coast; (Anomalous elements; Zn, Mn, Ni, Co and Hg)

West side of Port Bicobian in the central east coast; (Anomalous elements; Cu, Ni, Co and Hg)

West side of Dinatadmo Point in the southern part of the east coast; (Anomalous elements; Cu, Ni, Co and Hg)

Vicinity of the Dimakawal mineral showing in the southeastern part of the area; (Anomalous elements; Cu, Pb, Zn, As, Mn and Hg)

Of the above, the anomalies of the following five anomalous zones can be understood by the pressent knowledge regarding the respective geological setting, igneous activities and mineralization.

(1) North side of Capisayan in the northern part of the area Late Miocene to Early Pliocene Cabagan formation is distributed in this zone and stratified iron bed mineral showing are known. The anomalous elements are same to the cell to that of cell average values.

(3) Upstream of Tuguegarao River in the central mountain range; Diorite stocks which belong to the Northern Sierra Madre Batholith were intruded in this zone. Porphyry copper mineralization is assumed on the basis of the assemblage of anomalous elements. As compare with the cell average values, Cu and Cr anomalous cells are missing from this zone.

(4~5) West side of Port Bicobian in the central east coast; Cretaceous Dikinaraman Chert and Bicobian Basalt are exposed in this zone. Cyprus type massive sulfide and stratified manganese showings are known. Anomalous values of the above mentioned of elements are probably derived from these mineralizations. As compare with the cell average values, Mn and Cr znomalous cells are missing from this zone.

(6) West side of Dinatadmo Point in the southern part of the east coast: The Isabela ultramafic rocks are exposed in this zone, Ni, Co and Cr anomalous values are probably derived from the ultramafic rock. Several chromite mineral showings are known. As compare with the cell average values, Hg and Cr anomalous cells are missing from this zone.

(7) Surrounding area of the Dimakawal mineral showing in the southeastern part of the area; Early Oligocene Abuan Formation and diorite stocks which belong to the Northern Sierra Madre batholith are distributed in this zone. Several sulfide dissemination and vein type mineral showings are known. The anomalous values of the mentioned elements are probably derived from these mineralizations. As compare with the cell average values, As anomalous cells are containing to this zone.

3-2-2 Multivariate analysis

Factor analysis was carried out on each cell average values using the Varimax rotation method.

The content of silver was below detection limit in 99.9% the cells and thus this element was excluded from this analysis. Therefore, the elements used for factor analysis amount to ten; they are Cu, Pb, Zn, As, Mn, Ni, Co, Mo, Hg and Cr.

3-2-2-1 Correlation Analyses

At first, the correlation matrix (Table-12) between cell average values were solved, then eigen values and cumulative proportion of total variances were calculated.

It is clear that the cumulative proportion of total variance is reaches 83% up to the fifth factor of diagonal factor : 1. This means that the great portion of the dispersion of each value is covered up to No. 5 factor of diagonal factor : 1. On the other hand when SMC diagonal factor (Sequared multiple coefficient) is used on the correlation matrix, then another set of eigenvalues were calculated. These eigenvalues show positive value up to the sixth factor, but after the forth factor, eigenvalues show small amount.

From the above mentioned items, up to No. 5 factor were adopted for the factor analysis.

3-2-2-2 Interpretation of each factor

Five factors (Factor No. 1 to Factor No. 5) were adopted and used on the factor analysis. The left half of Table-13 shows factor loadings which were processed by main factor analysis (before rotation). The right half of Table-13 shows the factor loadings derived after adopting the Varimax Rotation Method Interpretations of each factor are as follows:

(A) Factor No. 1

With the exception of Mo factor loadings before rotation, are all positive especially Ni, Co, Cr and Mn, all have high factor loading value. These elements have the tendency to accumulate in ultramafic rock areas. Factor loading values after rotation indicate the distribution area of ultramafic rocks or specifically Ni, Co, Cr and Mn mineralizations.

(B) Factor No. 2

Factor loading values before rotation are negative for Cr, Ni and Co and positive for Cu, Pb, Zn, As and Mn. The former group has the tendency to accumulate into mafic rocks while the latter

Table-12 Correlation Matrix and Eigen Values

	Cu	Pb	Zn	As	Mn	Ni	Co	Mo	Hg	Cr
Cu	1.000									
Pb	0.198	1.000								
Zn	0.551	0.296	1.000							
As	0.163	0.262	0.191	1.000						
Mn	0.397	0.260	0.632	0.187	1.000					
Ni	0.114	−0.034	0.039	−0.004	0.238	1.000				
Co	0.240	−0.083	0.215	−0.059	0.486	0.827	1.000			
Mo	−0.009	0.153	−0.014	0.182	−0.122	−0.067	−0.070	1.000		
Hg	0.115	0.380	0.134	0.146	0.288	0.268	0.238	0.013	1.000	
Cr	−0.029	−0.056	0.012	0.031	0.168	0.888	0.716	−0.066	0.197	1.000

	Factor 1	Factor 2	Factor 3	Factor 4	Facto 5	Factor 6	Factor 7	Factor 8	Factor 9	Factor 10
Eigen Value Diagonal Factor: 1	3.124	2.153	1.296	0.973	0.777	0.579	0.543	0.333	0.147	0.075
C.P.T.V.	0.312	0.528	0.675	0.755	0.832	0.890	0.945	0.978	0.993	1.000
Eigen Value Diagonal Factor: S.M.C.	2.844	1.703	0.613	0.218	0.082	0.052	−0.058	−0.106	−0.204	−0.226

C.P.T.V.: Cumulative Proportion of Total Variance
S.M.C. : Squared Multiple Correlation

Table-13 Factor Loadings

Before Rotation						After Rotation						
Factor	1	2	3	4	5	Factor	1	2	3	4	5	Final Communality
Cu	0.450	0.513	−0.338	0.246	−0.127	Cu	0.032	−0.805	0.001	−0.085	0.027	0.656
Pb	0.231	0.596	0.438	−0.318	−0.139	Pb	−0.156	−0.233	0.767	−0.164	0.166	0.721
Zn	0.505	0.627	−0.340	0.135	−0.065	Zn	−0.005	−0.875	0.118	0.009	0.083	0.786
As	0.179	0.436	0.436	0.289	0.701	As	−0.009	−0.131	0.123	−0.090	0.973	0.987
Mn	0.689	0.414	−0.263	−0.070	0.036	Mn	0.253	−0.740	0.251	0.196	0.089	0.721
Ni	0.800	−0.517	0.140	0.066	0.006	Ni	0.961	−0.042	0.077	0.014	−0.004	0.932
Co	0.854	−0.358	−0.092	0.113	−0.098	Co	0.882	−0.311	0.013	0.033	−0.115	0.888
Mo	−0.086	0.179	0.595	0.604	−0.456	Mo	−0.032	0.033	0.061	−0.976	0.088	0.966
Hg	0.466	0.191	0.443	−0.563	−0.131	Hg	0.240	−0.042	0.848	0.066	0.004	0.784
Cr	0.716	−0.562	0.191	0.078	0.102	Cr	0.932	0.066	0.036	0.030	0.078	0.881

group seems to be concentrated into acidic rocks. From these facts, the No. 2 factor seems to show the grouping nature for the contrasting behavioral elements. Factor loadings after rotation show remarkable negative values for Cu, Zn and Mn. This factor indicate Cu, Zn and Mn mineralizations.

(C) Factor No. 3
Each factor loading after rotation is positive for all elements. The high factor loading values of Hg and Pb indicate Pb and Hg mineralizations and associated alteration significant.

(D) The factor No. 4
Factor loading values after rotation are shown visible negative value for Mo indicate Mo mineralization.

(E) Factor No. 5
Factor loading values after rotation shows visible positive value for As. From this Factor No. 5 data, it is indicates As distribution behavior.

From these interpretations, the following factors seem to be important with respect to some particular elemental distributions.

(a) Factor No. 1 after rotation indicate Ni, Co, Cr and Mn mineralizations.

(b) Factor No. 2 after rotation indicate Cu, Zn and Mn mineralizations.

(c) Factor No. 3 after rotation indicate Pb mineralization

(d) Factor No. 4 after rotation indicate Mo mineralization

3-2-2-3 Distribution of the geochemical anomalies

The factor score of each grid is calculated by mutipliying the cell average value of each element and the factor score coefficients, summarizing them for every cell. The statistical procedure is carried out on all these factor scores.

These factor scores are classified based on the following ranks and are plotted on a 1:1,000,000 topographic map.

Since Factor No. 2 is negative values for Cu, Zn and Mn factor loadings after rotation and Factor No. 4 shows a negative value on Mo factors loading after rotation, another classified rank is adopted for these negative values.

	Frequency		Frequency
A	$90\% \leqq Z < 100\%$	A	$0\% \leqq Z < 10\%$
B	$80\% \leqq Z < 90\%$	B	$10\% \leqq Z < 20\%$
C	$70\% \leqq Z < 80\%$	C	$20\% \leqq Z < 30\%$
D	$50\% \leqq Z < 70\%$	D	$30\% \leqq Z < 50\%$
E	$0\% \leqq Z < 50\%$	E	$50\% \leqq Z < 100\%$

(Adopted for Factor No.1,2,3 and 5) (Adopted for Factor No.2 and 4)

Attached plates 2-5-1 to 2-5-5 show the areal distribution of these anomalous values. The concentrated areas of each anomalous values are as follows.

(A) Factor No. 1 (Expressed close relation to Co, Ni and Cr anomalies.)
Whole ophiolite region east side the Divilacan thrust.
Distribution area of Callao Limestone and Cabagan Formation.

(B) Factor No. 2 (Expresses close relation to Cu, Zn and Mn anomalies.)
North side of the Capisayan mineral showing in the northern part.
West side of Awang Cove in the northern east coast. Upstream of Tuguegarao River in northern part.
Ophiolite distribution area south of Divilacan Bay.
West side of Port Bicobian in the central east coast.
Surrounding part of Dimakawal mineral showing in the southeastern part of the area.

(C) Factor No. 3 (Expresses close relation to Hg and Pb anomalies.)
Central to southern portion of the central mountain range.
Southern part of the eastern coast.

(D) Factor No. 4 (Expresses close relation to Mo anomalies.)
Diorite intruded area west of Awang Cove in the east coast.
Diorite intruded area upstream of Tuguegarao River.
Surrounding area of the Bicobian mineral showing.

(E) Factor 5 (Expresses close relation to As Anomalies.)
Distribution area of Abuan, Callao Limestone and Cabagan Formation in the middle to the northern part of the area.
Vicinity of Palanan and Kanaipang limestone in the east coast and Dimakawal mineral showing in the southeastern part of the area.

3-3 Analyses of Heavy Mineral Samples

3-3-1 Univariate analyses of the analytical results of the panned samples.

A total of 370 panned samples were collected from the Northern Sierra Madre Area. Au, Ag and Ga analyses were carried out.
Univariate analyses of these results were done.

Table-14 Basic Statistical Values of Panned Samples

	Au (ppb)	Ag (ppb)	Ga (ppm)
$\bar{X}$	31	75	12
$\bar{X}+1.0\sigma$	282	184	18
$\bar{X}+1.5\sigma$	857	287	22
$\bar{X}+2.0\sigma$	2,604	448	27
Maximum	4,600	650	33
Minimum	<20	<100	<2
Deteaction limit	20	100	2
Ratio below D.L.	95%	89%	5%

$\bar{X}$; Mean value σ; Standard deviation D.L.; Detection limit

Those over $\overline{X}+1.0\sigma$ values are plotted based on the following classification utilizing each element symbol on a 1 : 1,000,000 scale areal map.

Range	Rank	
$\overline{X}+2.0\sigma \leq Z$	A	◎
$\overline{X}+1.5\sigma \leq Z < \overline{X}+2.0\sigma$	B	○
$\overline{X}+1.0\sigma \leq Z < \overline{X}+1.5\sigma$	C	○

The locality map of the anomalous values indicates the following distribution tendencies.

(1) A, B and C ranks of Au samples are located at the southern part of the central mountain range and overlap with the anomalous zones of Cu, Pb, Zn, Mn and Hg cell average values.

(2) A, B, and C ranks of Ag samples overlap Au anomalous zones and are located around the diorite stock at southwestern Bolos Cove in the northern east coast. These anomalies were also noted to be associated with Cu, Pb, Zn, As and Mo cell average anomalous zones.

(3) A and B rank of Ga samples located along the boundary zone between the Ibulao Limestone and the Dibuluan Formation in southeastern Cauayan, in the Dibuluan Formation at the east side of Tuguegarao and in the Dipadian Formation at the southern part of the Divilacan Bay. Zn cell average anomalous zone overlap at the southeastern Cauayan area while the Ga anomalies were observed to be associated with Cu, Zn, Mn, Ni, Co and Cr cell average anomalous zones at the southern part of the Divilacan Bay.

3-3-2 Modal analyses for the identified minerals of panned samples.

Forty panned samples were selected at random from the 370 panned samples, the component minerals were identified with binocular microscope in PETROLAB. Attached plate-4 shows each heavy mineral ratio (Wt %) to total amount of heavy minerals with the circular graph and number in small central circle showing total heavy mineral ratio (Wt %) to whole sample.

The panned samples consisted of the following minerals with their corresponding average weight (%), which are shown in Table-15.

3-3-2-1 Areal distribution of heavy minerals

The weight percent of heavy minerals in the panned samples are plotted on a 1 : 1,000,000 areal map with circuls indicating each sampling point. (Plate-4)

The panned samples are roughly divided three groups on the basis of its heavy mineral ratio to whole sample, namely, 73-98% group, 53-68% group and 16-26% group. Each group is distributed in a certain particular region.

(1) Group of 73-98% heavy mineral ratio: In this group, magnetite and chromite are the major heavy minerals and a negative correlation is observed between the two. This group id distributed in the ophiolite basement of the eastern part of the survey area and the central mountain range which consists of the pyroclastics of the Abuan Formation and intruded diorite stocks.
Heavy mineral ratio is high in the eastern part, northern and southern part of the area. The central part of the mountain range shows variable ratio.

(2) Group of 53-68% heavy mineral ratio: Magnetite and chromite are the major minerals, samples which show over 60% heavy mineral ratio exhibit a negative correlation between the two minerals. The samples of this group are distributed along the western slope of the central mountain range.

(3) Group of 16-26% heavy mineral ratio: The heavy mineral ratio of this group shows a considerable range and correlation among heavy minerals is not observed. This group is mainly distributed at the transition boundary between the mountain range and basin. Such places used to be composed of various kinds of sediments, explaining why the heavy mineral contents noted were not high.
The correlation coefficients of these constituent minerals of the panned samples are shown in Table-16.

Table-15 Major Constituent Mienrals and Average Wt.% of the Panned Samples

	Heavy Minerals						Rock Forming Minerals					
Mineral	Magnetite	Chromite	Ilmenite	Rutile	Fe Mineral	Zircon	Olivine	Pyroxene	Hornblend	Feldspar	Quartz	Others
Code	mt	cm	il	ru	Fe	Z	ol	P	Ho	F	Q	oth
Average Wt.%	49.46%	17.64%	3.62%	0.03%	5.21%	0.26%	3.62%	7.59%	4.56%	5.91%	1.99%	0.31%

Table-16 Correlation Coefficients of the Constituent Minerals of the Panned Samples

	mt	cm	il	ru	Fe	Z	Ol	P	Ho	F	Q	Oth
mt	1.00											
cm	− 0.47	1.00										
il	− 0.07	0.06	1.00									
ru	0.12	− 0.05	− 0.03	1.00								
Fe	− 0.52	0.22	− 0.37	− 0.01	1.00							
Z	− 0.20	0.01	0.52	− 0.07	− 0.08	1.00						
Ol	− 0.46	− 0.19	0.42	− 0.13	0.21	0.51	1.00					
P	− 0.42	− 0.40	− 0.25	− 0.13	0.28	0.03	0.25	1.00				
Ho	− 0.23	− 0.42	− 0.11	0.11	− 0.13	− 0.03	0.11	0.45	1.00			
F	− 0.52	− 0.40	− 0.25	− 0.09	0.26	− 0.08	0.40	0.75	0.63	1.00		
Q	− 0.52	− 0.40	− 0.07	− 0.07	0.33	0.02	0.63	0.60	0.55	0.87	1.00	
Oth	− 0.35	− 0.20	− 0.18	− 0.04	0.28	− 0.10	0.38	0.37	0.09	0.61	0.59	1.00

Oth : Other minerals

4. Correlation with Existing Regional Data

The compilation of the gravimetric map, and extraction of the lineaments from LANDSAT image analysis were carried out during the first fiscal year (1984) of this project.

These data, as presented in this report, were plotted on a 1 : 1,000,000 scale topographic maps (attached Plate-5, Plate-6) and were analysed in terms of its significance and relation-ship with the results of both the geological and geochemical surveys.

4-1 Lineament Data (Attached Plate-6)

LANDSAT image analyses were carried out by both JICA-MMAJ and the counterpart Philippine agency (DENR) simultaneously 1985.

Plate-6 combines these two lineament data sources using different colors.

The Divilacan thrust which divides the survey area into two terranes, east and central terrane is clearly observed with the N-S trending formation boundaries reflecting the N-S trending lineaments. The eastward curveture of the lineament is reflected at the Dibuluan and Cabagan Formations at the southeastern Ilagan area.

The Paret embayment structure at eastern Tuguegarao is reflected as a combination f SW-NE, N-S and E-W lineaments at the corresponding locality.

4-2 Gravity Data (Attached Plate-5)

In the Northern Sierra Madre area, gravity data (Bouguer anomaly) carried out by MGB since 1966 are available for the whole area the attached plate-5 shows Buoguer anomaly with 10 milligal contour.

The contour lines a show south to north trend. The east side is characterized high anomalies which the west side has low anomalies in general. These tendencies are inferred to reflect the distribution of the lithologies and the geological structures of this area the high density ophiolite located at the eastern side and low density younger sediments at the western side gradually increasing in quantity up to the Cagayan River.

Along the Cagayan River, the negative Bouguer anomaly noted is a reflection of the Cagayan Valley syncline structure.

5. Correlation between the Surveyed Mineral Showings and Geochemical Anomalies

The correlation between the surveyed mineral showings in the Northern Sierra Madre Area and the results of analyses of the geochemical data processed by various methods is shown in Table-17.

From this table, it is clear that Ni, Co and Cr anomalous cells are associated closely with chromite mineral showings while Cu, Pb, Zn, As, Mn and Hg, etc., anomalous cells are associated closely with copper mineral showings.

As for the anomalous cells of the factor analyses, anomalous cells of Factor No. 1 are associated with Mn, Cr and Cu mineral showings, on the contrary, anomalous cells of Factor No. 2 are associated with Cu and Mn mineral showings. Anomalous cells of Factor No. 3 are associated with Mn, Cu and Au mineral showings and also with partly Cr mineral showings.

Anomalous cells of Factor No. 4 are usually distributed with in and around the Northern Sierra Madre Batholith, therefore, some porphyry copper type mineralizations can be expected within these localities.

Anomalous cells of Factor No. 5 are related to As anomalous cells, suggesting close finity to vein and strata-bound type mineral showings.

Table-17 Relationship between Mineral Showings and Geochemical Anomalies

Index		Mineral Showings Name	Commodity	Cell Average Analysis											High-pass Filter Analysis											Factor Analysis				
	No.			Cu	Pb	Zn	Ag	As	Mn	Ni	Co	Mo	Hg	Cr	Cu	Pb	Zn	Ag	As	Mn	Ni	Co	Mo	Hg	Cr	No.1	No.2	No.3	No.4	No.5
EASTERN PART	9	Dikadiaoan	Mn	–	–	–	–	–	–	◎	–	–	–	◎	–	–	–	–	–	–	–	–	–	–	–	○	–	◎	–	–
	17	Disawit	Mn	–	–	–	–	–	–	◎	–	–	–	◎	–	–	–	–	–	–	–	–	–	–	–	○	–	◎	–	–
	26	Kanaipang Hill	Mn	–	–	–	–	◎	–	◎	–	–	◎	◎	–	–	–	–	–	–	○	–	–	○	–	–	○	◎	–	–
	28	Bicobian	Cu	◎	–	–	–	–	◎	◎	◎	–	◎	–	◎	–	–	–	–	–	–	–	–	○	–	○	–	◎	◎	–
	34	Cas Chrome Wasayan I	Cr	–	–	–	–	–	◎	◎	◎	–	–	◎	–	–	–	–	–	–	○	◎	–	–	◎	◎	–	◎	–	–
	35	Cas Chrome Wasayan II	Cr	–	–	–	–	–	–	◎	◎	–	–	◎	–	–	–	–	–	○	◎	◎	–	–	○	◎	–	–	–	–
	39	Dikapisan	Cr	–	–	–	–	–	–	◎	◎	–	–	◎	–	–	–	–	–	–	–	–	–	–	–	◎	–	◎	–	–
	43	Dibenelang	Cr	–	–	–	–	–	–	◎	–	–	–	◎	–	–	–	–	◎	–	–	–	–	–	◎	○	–	–	–	–
	44	Iacson	Cu	◎	–	–	–	–	○	◎	◎	–	◎	◎	–	–	–	–	–	–	–	–	–	–	○	◎	–	◎	◎	–
	46	Disukad	Cr	–	–	–	–	–	–	◎	◎	–	–	◎	–	–	–	–	–	–	–	–	–	–	○	◎	–	–	◎	–
	47	Dilacnadinom	Cr	–	–	–	–	–	–	◎	◎	–	◎	◎	–	–	–	–	–	–	–	–	–	–	–	◎	–	–	◎	–
WESTERN PART	6	Menuma	Cu	–	–	–	–	–	–	–	–	–	–	–	–	–	–	–	–	–	–	–	–	–	–	–	◎	–	–	–
	7	Siagot	Cu	–	–	–	–	–	–	–	–	–	–	–	–	–	–	–	–	–	–	–	–	–	–	–	◎	–	–	–
	8	Ilagan	Cu	–	–	–	–	–	–	–	–	–	–	–	–	–	–	–	–	–	–	–	–	–	–	–	◎	–	–	–
	11	Isabela	Cu	–	–	–	–	–	–	–	–	–	–	–	–	–	–	–	–	–	–	–	–	–	–	–	–	–	–	–
	(14)	Casablangan	Cu	–	–	–	–	–	–	–	–	–	–	–	–	–	–	–	–	–	–	–	–	–	–	–	–	–	◎	–
	(15)	Dinacdacan	Cu	–	–	–	–	–	–	–	–	–	–	–	–	–	–	–	–	–	–	–	–	–	–	–	–	◎	◎	–
	(16)	Capisayan West	Fe	–	–	–	–	○	–	–	–	–	–	–	–	–	–	–	–	○	–	–	–	–	–	–	–	–	–	○
	(17)	Capisayan East	Fe	–	–	–	–	–	–	–	–	–	–	–	–	–	–	–	○	○	–	–	–	–	–	–	–	–	–	◎
	19	Dimakawal	Mn, Cu	◎	◎	◎	◎	◎	◎	◎	–	–	◎	–	◎	○	◎	–	◎	◎	–	–	–	–	–	–	–	◎	–	◎
	37	Dinapiqui	Cu, Au	◎	◎	◎	–	◎	◎	–	–	–	◎	–	◎	○	–	–	–	–	–	–	–	–	–	–	–	◎	○	◎
	38	Dimatatno	Cu	–	–	–	–	–	–	◎	○	–	–	◎	–	–	–	–	–	–	◎	–	–	–	○	◎	–	–	–	–
	41	Giwed	Cu	–	–	–	–	◎	–	◎	–	–	–	◎	○	–	–	–	○	–	–	–	–	–	–	◎	–	–	–	◎
	42	Diudenan	Cu	–	–	–	–	–	–	◎	–	–	–	◎	○	–	–	–	–	–	◎	–	–	–	○	◎	–	–	–	◎
	45	Bolos River	Cu	–	–	–	–	◎	–	◎	–	◎	–	–	–	–	–	–	○	–	–	–	○	–	–	○	◎	–	–	–
	48	Disdo Creek	Au	–	–	–	–	–	–	–	–	–	–	–	–	–	–	–	–	–	–	–	–	–	–	–	–	–	◎	–
	49	Dina Creek	Cu	–	–	–	–	–	–	◎	–	–	–	–	–	–	–	–	–	–	–	–	–	–	–	–	–	–	○	–
	50	Diwagao	Au, Cu	–	–	–	–	–	–	–	–	–	–	–	–	–	–	–	–	–	–	–	–	–	–	–	◎	◎	–	–
	51	Dicamay River	(?) Fe	○	–	◎	–	–	–	–	–	–	–	–	–	–	○	–	–	–	–	–	–	–	–	–	–	–		
	52	Ilagan River	(?) Au	–	–	◎	–	–	–	–	–	–	–	–	–	–	–	–	–	–	–	–	–	–	–	–	–	–		
	53	Diden River	(?) Au, Ag	–	–	–	–	–	–	–	–	–	–	–	–	–	–	–	–	–	–	–	–	–	–	–	–	–		
	54	Palig Creek	(?) Cu, Au	◎	◎	◎	–	◎	◎	◎	–	–	◎	–	◎	○	○	–	◎	◎	–	○	–	–	–	–	–	◎		

◎ : Mineral showing locates in the over $\overline{X}+1.5\sigma$ value cell
○ : Mineral showing locates in the $\overline{X}+1.0\sigma \sim \overline{X}+1.5\sigma$ value cell
– : Mineral showing locates in the below $\overline{X}+1.0\sigma$ value cell

6. Evaluation and Conclusions

6-1 Consolidated Evaluation of the Survey Results

6-1-1 Geology and structures

The Northern Sierra Madre Area is located from the Eastern Physiographic Province to the Central Physiographic province in Northern Luzon. Although most of the area falls under the jurisdiction of the Isabela Province - Region II, the northern part of the area belongs to the Cagayan Province.

The survey area is divided by the N-S trending Divilacan Thrust, which extends through the Divilacan Bay, into two tectonic areas namely the Eastern Part and the Western Part.

6-1-1-1 The eastern part

The basement rock of this area is an ophiolite suite, the Isabela Ultramafic Complex, which consists mostly of peridotite accompanied by lenticular dunite and gabbro of massive and cumulative shapes. The ultramafic rocks sometimes host chromite ore deposits.

The Bicobian Basalt and the Dikinamaran Chert unconformably cover unconformably the Ultramafic Complex.

The Dierico and Palanan Formation of Miocene age and Pliocene to Pleistocene Kanaipang limestone overlie unconformably the basement rocks as Tertiary forearc sediments.

The igneous activity in this area is related to oceanic crust formation which is thought to be responsible for the formation of the Bicobian Basalt during the Cretaceous.

6-1-1-2 The western part

The basement rocks of the Western Part are composed of Late Eocene to Middle Oligocene basaltic to dacitic lava flows, pyroclastics,l volcanic wacke and conglomerates.

These basement rocks are widely distributed at the central mountain range.

The Northern Sierra Madre Batholith intruded the Middle Oligocene to Late Oligocene sedimentary rocks as dioritic to granodioritic stocks or cupolas.

The Late Oligocene Dibuluan Formation which consists of basaltic flow and pyroclastics unconformably covers all the above mentioned rocks.

The Lubuagan Formation of flysh type turbidite overlies unconformably the Late Miocene Callao Limestone which in turn covers the Dibuluan Formation unconformably.

The Late Miocene Callao limestone is interbedded at the lower part with the Lubuagan Formation and at the upper part with the Cabagan turbidite.

The uppermost formation of the Western Part is the Plio-Pleistocene Ilagan Formation which is composed of bedded but poorly compacted sandstone, shale and polymictic conglomerates.

The central mountain range is a magmatic arc, and the Cagayan River basin which lies in the west side of it is a typical backarc basin, where various sediments after the deposition of the Masipi Green Tuff show a gentle monoclinic structure dipping west.

The main igneous activity is the Late Oligocene Northern Sierra Madre Batholith intrusion which occurred in a N-S direction as suggested by the distribution of the dioritic stocks.

Aside from this activity, other igneous activities are known to have occurred as evidenced by the Late Eocene to the Middle Oligocene basaltic and dacitic rocks and Late Oligocene basaltic activities.

6-1-1-3 Geological structures

The evaluation of geology and structures of the Northern Sierra Madre area are intimately associated with the subduction events along its eastern coast.

This subduction is believed to have begun in the Eocene and had ceased in the Late Oligocene and was reactivated during the Holocene. The subduction occurred in the East Luzon Trough.

6-1-2 Mineralizations

Four principal types of mineralization have been recognized in the Northern Sierra Madre area as follows:

(A) Orthomagmatic mineralization: Chromium and nickel mineralizations occur in the Isabela ultramafic rocks of the Eastern Part.

(B) Cyprus-type massive sulfide mineralization: Massive sulfide mineralization occurs in the boundary of the Cretaceous Bicobian Basalt and Dikinamaran Chert.

(C) Copper sulfide disemination in the volcanic breccia associated with the Oligocene basalt: This mineralization occurs in the volcanic breccias associated with the basalt flow of the Abuan Formation and accompanying hydrothermal alteration zones.

(D) Porphyry copper type mineralization: Sulfide disseminations at the contact of the Northern Sierra Madre Batholith and andesite to dacite which belong to the Abuan and the Mt. Cresta Formations.

6-1-3 Geochemical Analyses

Anomalous zones are selected from anomalous cells which are defined by geochemical analysis methods utilizing the following standards.

A. Each anomalous zone should more or less be defined by two detected element anomalous values.

B. Each anomalous zone should at least be suggested by over two methods of geochemical analyses.

Table-18 Relation between the Extracted Anomalous Zones and Results of Geochemical Analyses

No.	Extracted anomalous zones	Location	Cell average value										Highpass filter value										Factor analysis					Geological setting and mineralization
			Cu	Pb	Zn	Ag	As	Mn	Ni	Co	Hg	Cr	Cu	Pb	Zn	Ag	As	Mn	Ni	Co	Hg	Cr	1.	2.	3.	4.	5.	
1	North side of Capisayan (Northern part of the area)	121°54' E 18°02' N	○		○			○					○		○			○						○				Capisayan mineral showings (16), (17) (Pliocene iron rich bed) were known
2	West side of Awang Cove (The east coast)	122°06' E 17°41' N		○					○					○				○	○					○		○		Porphry copper mineralization associated with diorite stocks is expected
3	Upstream Tuguegarao River	122°00' E 17°37' N	○		○		○							○	○		○							○	○	○		ditto
4	South side of Divilacan Bay (The central east coast)	122°18' E 17°15' N	○		○			○	○	○	○	○	○		○			○	○	○	○			○			○	Many mineral showings were known in this ophiolite region
5	West side of Port Bicobian (The central east coast	122°24' E 17°16' N	○					○	○	○	○	○							○	○	○			○		○		ditto
6	West side of Dimatadmo Point (The southern east coast)	122°18' E 16°35' N							○	○	○	○							○	○			○		○			Chromite mine is developed associated with Isabela Urtramafic Complex
7	Around part of Dimakawal mineral showing (Southeastern edge of the area)	122°13' E 16°35' N	○	○	○			○			○		○	○	○		○	○			○			○	○	○	○	Dimakawal mineral showing (19) associated with basalt lava of Abuan Formation was observed

○ : Elements concerned anomalous zone.

Table-18 shows the anomalous zones selected based on the above standards and relevant features of each anomalous zone.

6-1-4 Evaluation of the anomalous zones

(1) Northern part of Capisayan mineral showing in the northern part of the area:
This anomalous zone is inferred to have been derive from the magnetite-rich bed in the Pliocene sediments which was observed at Capisayan. The assay results of this bed are not high, so this zone is excluded from the promising zone.

(2) West side of Awang Cove in the eastern coast:
This zone has few elements which show anomalous values and is not included within the intruded zone of the Northern Sierra Madre batholith. Thus, this zone is excluded fro the Promising zone.

(3) Upstream of Tuguegarao River:
This zone has few elements which show anomalous value but an extensive alteration zone is observed around the diorite stocks at Casablangan (No. 14) and Dinacdacan (15) mineral showings, in which porphyry copper mineralization is expected. This zone is included in the promising zone (III).

(4) The south side of Divilacan Bay and the west side of Port Bicobian:
Both zones are located in an ophiolite region and elements show almost the same anomalous values. The west side of Port Bicobian which has Cyprus type mineralization is selected as a promising zone (II).

(5) The west side of Dinatadmo point in the eastern coast:
This zone is located in the surrounding area of Cas Chrome Wasayan I Mine which is under operation, therefore this zone is excluded from the promising zone.

(6) Vicinity of Dimakawal showing:
This zone has two types of mineralization, one is disseminated sulfied (Dimakawai (No. 19)) associated with basaltic lava of the Abuan Formation and the other is vein-type in altered andesite near the diorite stock (Palig Creek (54)). Anomalous values of the various elements are overlapped together, so this zone is included as a promising zone (I).

6-2 Conclusions

As a result of the consideration of the above mentioned available informations, three promising areas are selected with following priorities.

(I) Surrounding part of Dimakawal mineral showing (the southeastern most of the area):
Vein and dissemination type Mineralized zone in Eocene Basalt in Abuan Formation.
Assumed commodities are Cu, Pb and Zn.

(II) West side of Port Bicobian (the Central East Coast of the area):
Cyprus type massive sulphide mineralized zone which associated with strata-bound manganese in chert and lenticular chromite in ultramafic rocks locates in ophiolite of the Eastern Part.
Assumed commodities are Cu, Zn, Mn and Cr.

(III) Upstream of Tuguegarao River (the central mountain range):
Chloritization and sericitization zones accompanied pyrite impregnation at intrusive contact part between diorite and andesite of Abuan Formation, dacite of Mt. Cresta Formation Porphry copper type mineralization is expected.
Assumed commodities are Cu and Zn.

References

Aurelio, M. A., et al., 1987, *1ms., Tectonic Implications of the Geology and Mineral Resources of Northern Sierra Madre.

Balce, G. R., et al., 1980, Metallogenesis in the Philippines, Explanatory text for the CGMW Metallogenic Map of the Philippines, Metallogeny of Asia.

Bed, 1986, *2unpub., Sedimentary Basins of the Philippines: Their Geology and Hydrocarbon Potential.

BMG, 1981, Geology and Mineral Resources of the Philippines, vol.I

BMG, 1986, id vol.II

Caagusan, N. L. 1986, Source Material, Compaction History and Hydrocarbon Occurrences in the Cagayan Valley Basin, Luzon, Philippines, PNOC.

Caagusan, N. L. 1986, Stratigraphy of the Cagayan Valley Basin, 44p.

Cabantog, A. V. 1974, ms. Geological Field Verification of Copper manganese, etc., Deposits of Black Rock Mining Corporation in Barrio Dimakawal San Mariano, Isabela.

Christian, L .B., 1964 Post Oligocene Tectonic History of the Cagayan Valley Basin. The Philippines Geologist, vol.18, pp.114-147.

De Guzman, R., 1968, Geology of Bicobian, Port Area GSP, p.109.

DENR, 1985, Lineament Map from LANDSAT Imagely (1 : 250,000).

Durkee, E. F. and Pedersen, S. L., 1961, Geology of Northern Luzon, AAPG Bull., vol.45, pp.137-168.

Hamburger, M. W., Cardwell, R. K. and Isacks, B. L., 1983, Seismotectonics of the Philippine Island Arc. Edited by D. E. Hayes. The Tectonic and Geologic Evolution of Southeast Asian Seas and Islands Part 2, Edited by Hayes, D.E., pp.1-22.

JICA-MMAJ., 1987, Report on the Mineral Exploration - Mineral Deposits and Tectonics of two Contrasting Geologic Environments in the Republic of the Philippines. Phase III (Part I), the Northern Sierra Madre Area.

Jones, D. L., Howell, D. G., Coney, P. J. and Monger, J. W. H., 1983, Recognition, Charactor and Analysis of Tectonostratigraphic Terranes in the Western North America, Accretion Tectonics in the Circum-Facific Region, Edited by Hashimoto, M. and Uyeda, S. pp.21-35.

Karig, D. E., 1982, Accreted Terranes in the Northern Part of the Philippine Archipelago, Philippine SEATAR Committee Special Publication No.1, p.9-11.

Lewis, S. D. and Hayes, D. E., 1983, The tectonics of Northward Propagating Subduction Along Eastern Luzon, Philippine Islands, in the Tectonic and Geologic Evolution of Southeast Asian Seas and Islands, Part 2, pp.57-94.

McCabe, R. L., Almasco, J. N. and Yumul, G. P. Jr., 1985, Terranes in the Central Philippines, The Philippine Geologist, vol.39, No.1, pp.3-23.

Tamesis, E. V., 1976, The Cagayan Valley Basin - A Second Exploration Cycle is Warranted, SEAPAX Program, 21p.

Uyeda, S. and McCabe, R. L., 1982, A possible Mechanism of Episodic Spreading of the Philippine Sea, Geological Survey of Japan, Bulletin, Special Vol.1 No.1, pp.130-142.

Zanoria, A. S., Domingo, E. G., Bacuta, G. C. and Almeda, R. L., 1984, Geology and Tectonic Setting of Copper and Chromite Deposits of the Philippines, Geological Survey of Japan Report, No.263, pp.209-233 .

*1ms.; manuscript
*2unpub.; unpublished

PL-1 Geological Map and Section (1:1,000,000)

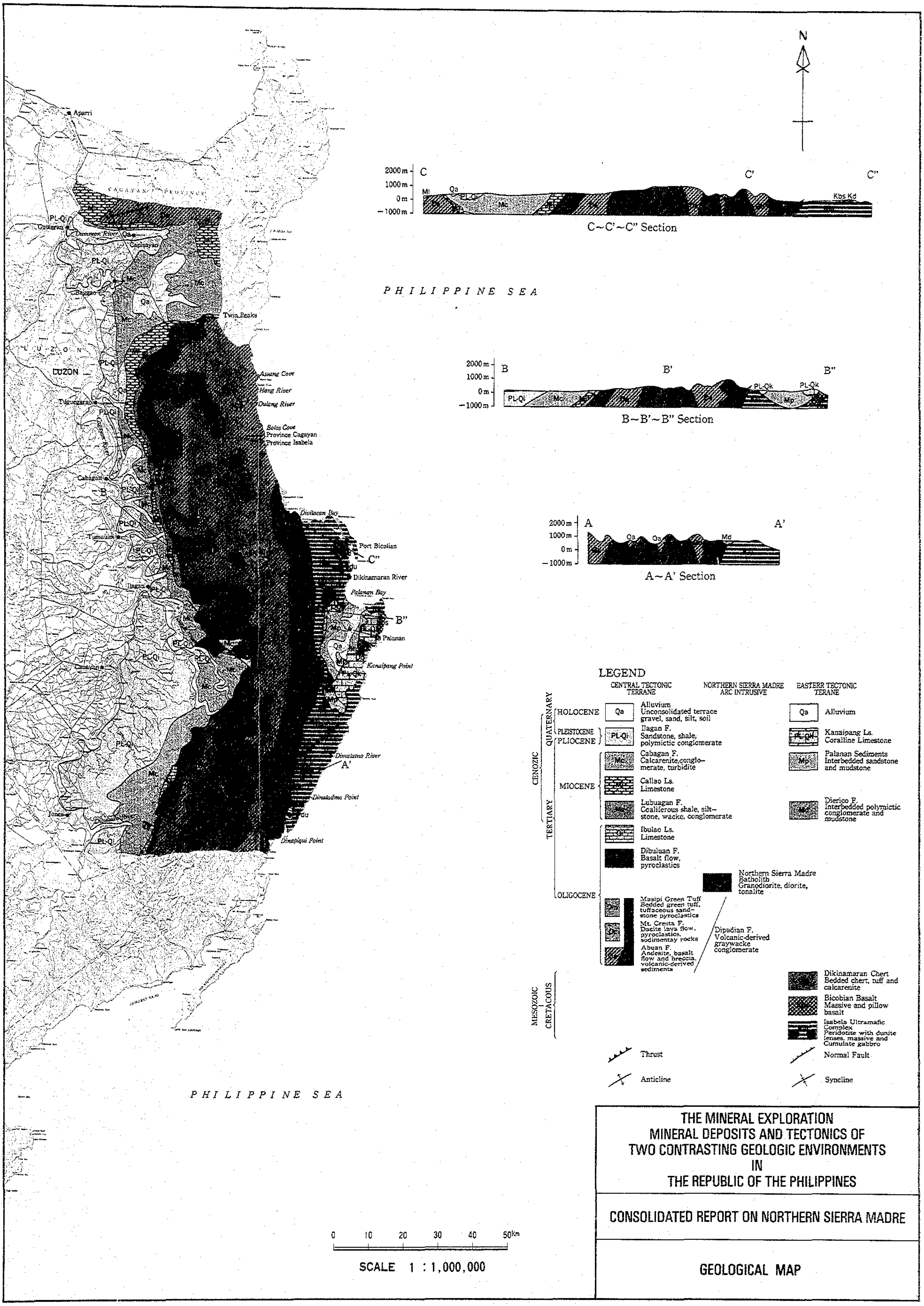

THE MINERAL EXPLORATION
MINERAL DEPOSITS AND TECTONICS OF
TWO CONTRASTING GEOLOGIC ENVIRONMENTS
IN
THE REPUBLIC OF THE PHILIPPINES

CONSOLIDATED REPORT ON NORTHERN SIERRA MADRE

GEOLOGICAL MAP

PL-2-1 (No. 1 to No. 10) Geochemical Analysis Cell Average Values Distribution Map (1:1,000,000)

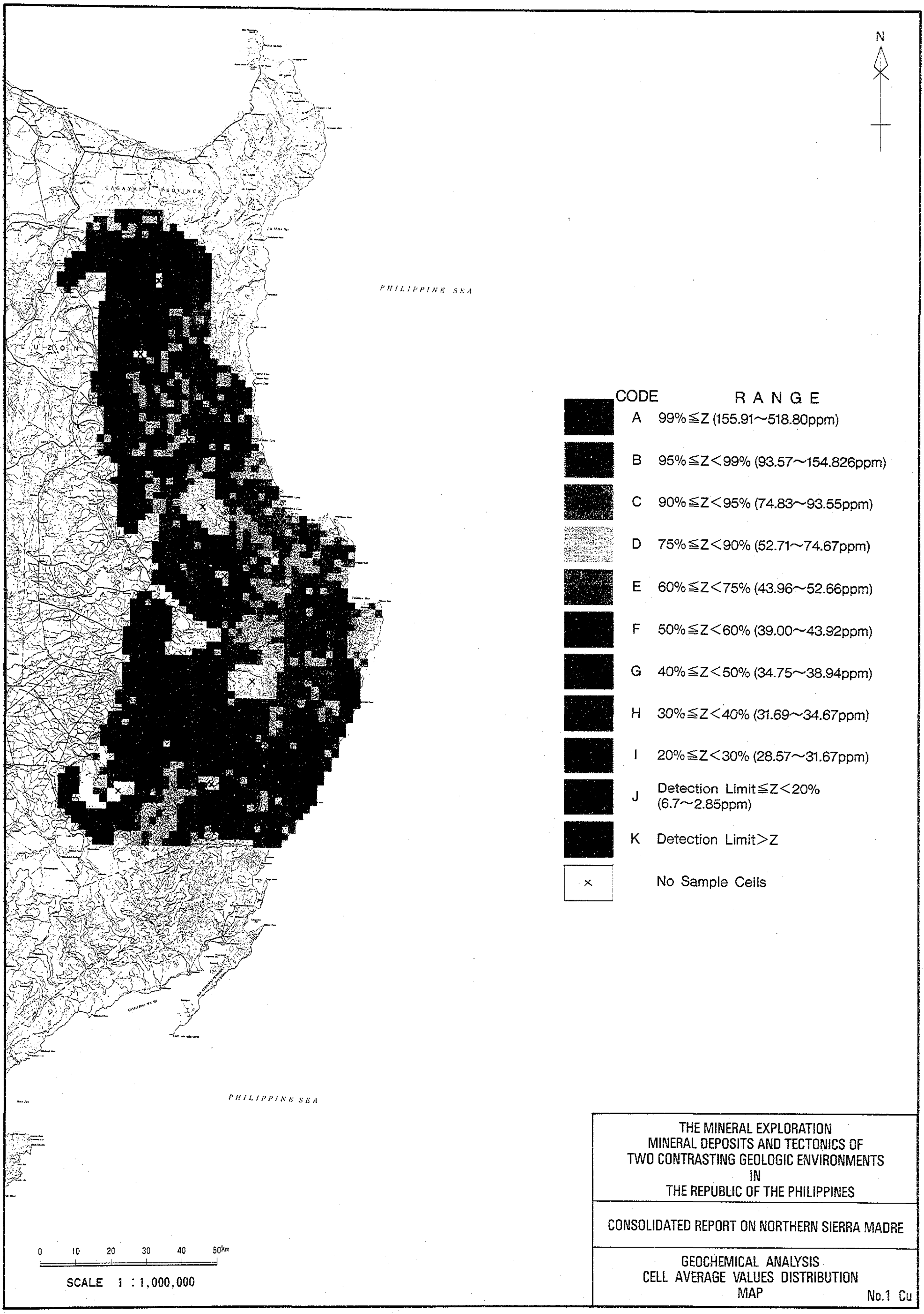

THE MINERAL EXPLORATION
MINERAL DEPOSITS AND TECTONICS OF
TWO CONTRASTING GEOLOGIC ENVIRONMENTS
IN
THE REPUBLIC OF THE PHILIPPINES

CONSOLIDATED REPORT ON NORTHERN SIERRA MADRE

GEOCHEMICAL ANALYSIS
CELL AVERAGE VALUES DISTRIBUTION
MAP

No.1 Cu

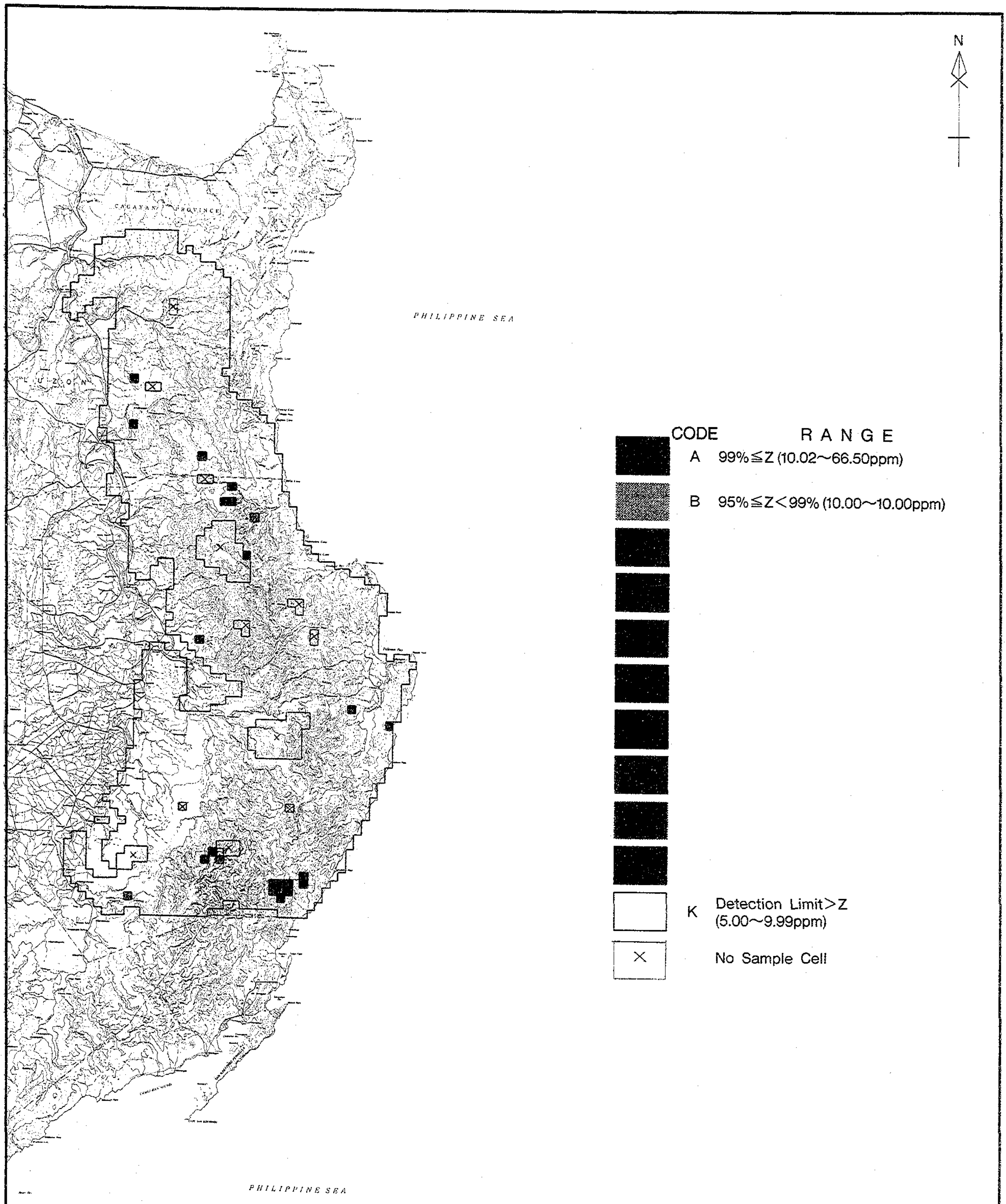

0 10 20 30 40 50km

SCALE 1 : 1,000,000

THE MINERAL EXPLORATION
MINERAL DEPOSITS AND TECTONICS OF
TWO CONTRASTING GEOLOGIC ENVIRONMENTS
IN
THE REPUBLIC OF THE PHILIPPINES

CONSOLIDATED REPORT ON NORTHERN SIERRA MADRE

GEOCHEMICAL ANALYSIS
CELL AVERAGE VALUES DISTRIBUTION
MAP

No.2 Pb

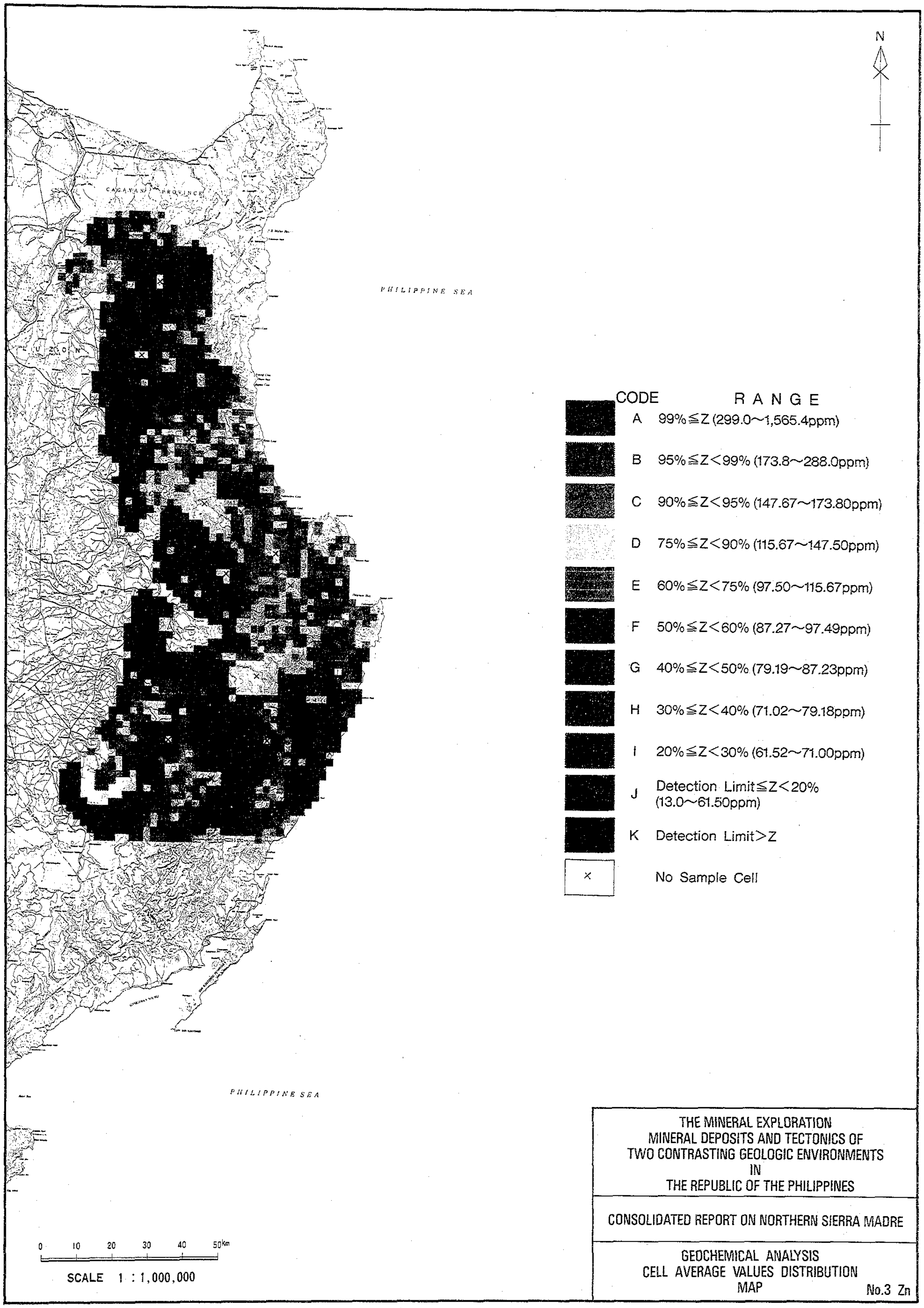

THE MINERAL EXPLORATION
MINERAL DEPOSITS AND TECTONICS OF
TWO CONTRASTING GEOLOGIC ENVIRONMENTS
IN
THE REPUBLIC OF THE PHILIPPINES

CONSOLIDATED REPORT ON NORTHERN SIERRA MADRE

GEOCHEMICAL ANALYSIS
CELL AVERAGE VALUES DISTRIBUTION
MAP

No.3 Zn

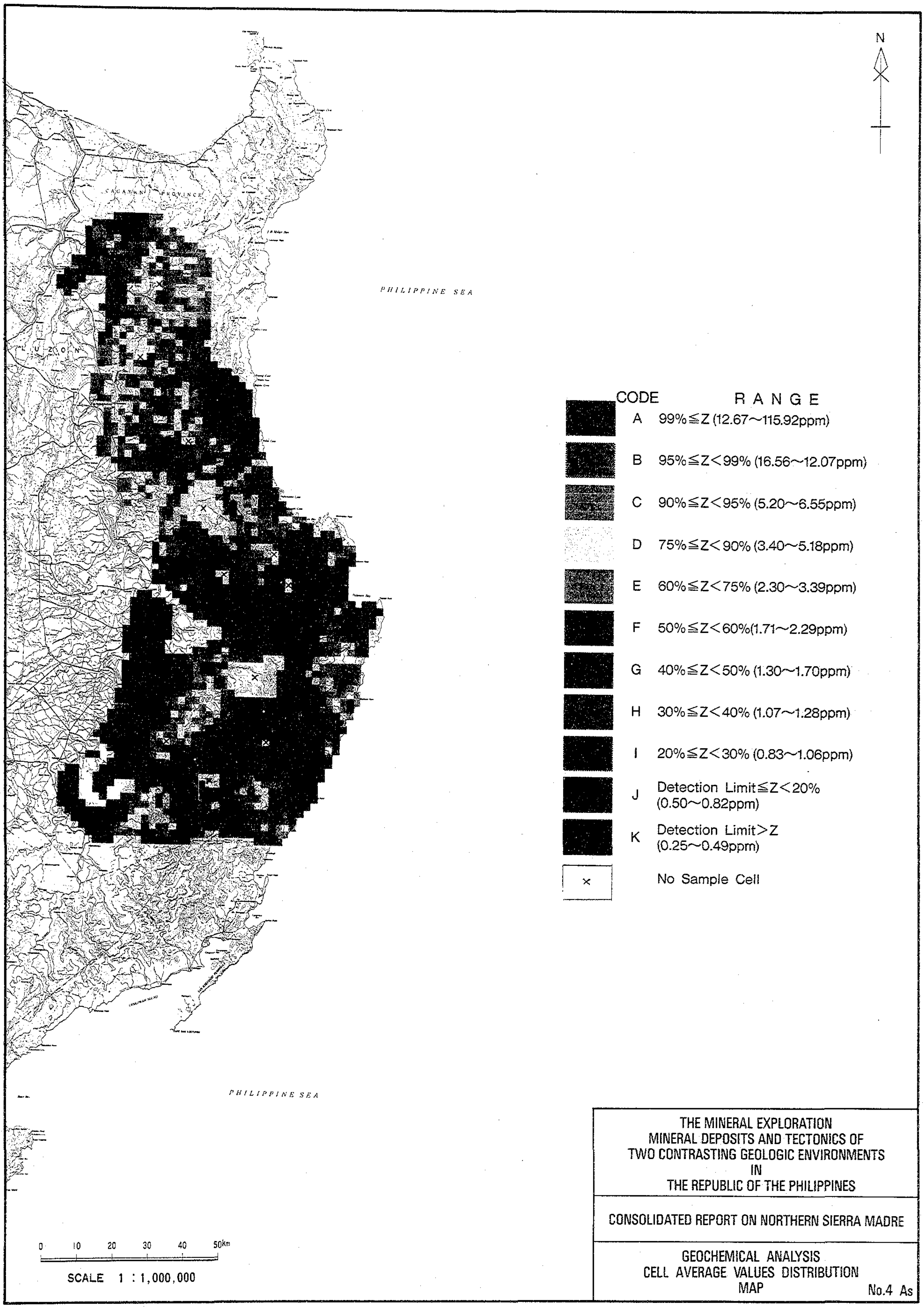
N
PHILIPPINE SEA
PHILIPPINE SEA
CODE RANGE
A 99%≦Z (12.67~115.92ppm)
B 95%≦Z<99% (16.56~12.07ppm)
C 90%≦Z<95% (5.20~6.55ppm)
D 75%≦Z<90% (3.40~5.18ppm)
E 60%≦Z<75% (2.30~3.39ppm)
F 50%≦Z<60%(1.71~2.29ppm)
G 40%≦Z<50% (1.30~1.70ppm)
H 30%≦Z<40% (1.07~1.28ppm)
I 20%≦Z<30% (0.83~1.06ppm)
J Detection Limit≦Z<20% (0.50~0.82ppm)
K Detection Limit>Z (0.25~0.49ppm)
× No Sample Cell
0 10 20 30 40 50km
SCALE 1 : 1,000,000
THE MINERAL EXPLORATION
MINERAL DEPOSITS AND TECTONICS OF
TWO CONTRASTING GEOLOGIC ENVIRONMENTS
IN
THE REPUBLIC OF THE PHILIPPINES
CONSOLIDATED REPORT ON NORTHERN SIERRA MADRE
GEOCHEMICAL ANALYSIS
CELL AVERAGE VALUES DISTRIBUTION
MAP
No.4 As